SEMINAR ON
NUCLEAR MEDICINE AND RADIOTHERAPY
1992 - 1993

(FOLLOW UP TEAM FOR THE GROUP TRAINING COURSE IN MEDICAL AND BIOLOGICAL APPLICATION OF RADIATION AND RADIOISOTOPES)

VOL. I (NUCLEAR MEDICINE)

JAPAN INTERNATIONAL COOPERATION AGENCY

NATIONAL INSTITUTE OF RADIOLOGICAL SCIENCES

Status of General Nuclear Medicine in Japan

Fumio SHISHIDO, M.D.

Toshiro YAMASAKI, M.D.

Division of Clinical Research

National Institute of Radiological Sciences

9-1, Anagawa 4-chome, Inage-ku, Chiba, 263

JAPAN

Introduction

Clinical nuclear medicine is common in Japan, and almost all of them are conventional one. But nowadays PET facilities are increasing in number in this country (Table 1). Until now, this modality is available in 19 institutions. Using this technic, it has been possible to measure regional blood flow, energy metabolism, receptor density and so on, in living human beings. The recent upsurge in interest in PET studies seems to be due to success in the noninvasive measurement of regional neuroreceptor density in the brain (Figure 1). Another trend in nuclear medicine is radioimmunoimaging. But it is necessary to resolve the problem to use animal protein as a monoclonal antibody, for using this technic in clinical nuclear medicine.

Today I don't want to present data of these ultramodern modalities, but show the present status of conventional nuclear medicine in Japan.

1.Nuclear medicine facilities

Number of nuclear medicine facilities in Japan are shown in Table 2.
478 hospitals practice both in-vivo and in-vitro examinations in 1991. Hospitals which practice only in-vivo examinations were 672 in number, also in last year. Regarding to in-vitro test, the facilities can be categorized as hospitals and private assay laboratories. Facilities which practice only in-vitro studies were 103 in number altogether, in 1991.

2. Radionuclides and cold kids used for in-vivo studies

Radionuclides used for in-vivo procedures in one year are shown in Table 3. The most frequently used radionuclides for in-vivo examinations was Tc-99m. Other frequently used radionuclides were Xe-133, Ga-67, Tl-201 and I-123. Variations in the amount of representative radionuclides used per year are shown in Figure 2. We can see a rapid growth in the amount of pertechnetate solution and Tl-201 chloride during recent 2 or 3 years.

Table 4 shows the amount of cold kits used for labeling Tc-99m per year.

3.Test tubes used for in-vitro studies

Test tubed used for in-vitro studies in number per year are shown in Table 5. Regarding to in-vitro test, we must pay attention to its decrease in number.

4. Total number and frequency of in-vivo examinations

During 2 months of June 1982 and June 1987, 115870 and 121443 in-vivo nuclear medicine procedures were performed in 776 facilities in 1982 and 1043 facilities in 1987 respectively.They cover 86.6% of all hospitals which performed in-vivo procedures in 1982 and 92.5% of in-vivo institutes in 1987. Figure 3 shows the frequency of in-vivo examinations in 1982 and 1987. In 1982 the liver scintigraphy was performed most frequently, 23.8% of all in-vivo procedures. In 1987, the most frequent in-vivo examinations was the bone scintigraphy, which was 19.1%. The second test was tumor scintigraphy,and the third was liver scintigraphy. Anyhow liver scintigraphy was decreasing in number and frequency.

Nowadays single photon emission tomography, SPECT is common in nuclear medicine practice in Japan. Even in 1987, 8642 SPECT procedures were performed in one month, it was 7.1% of the total number of in-vivo examinations.

5. Numbers of in-vivo examinations per year in a medical college hospital

In Tokyo Women's Medical College Hospital, located in Tokyo, 6619 in-vivo nuclear examinations were performed in one year, from April 1989 to March 1990 (Figure 4). Also in this college hospital, the bone scintigraphy was performed most frequently as shown in the figure. The next 5 tests were myocardial imaging by Tl-201 chloride, tumor scintigraphy with Ga-67 citrate, renal test using Tc-99m DTPA, lung perfusion study and cardiovascular dynamic imaging. On the contrary the liver scintigraphy was done only in 18 cases in that year.

6. Internal use of unsealed radioisotopes for therapy

Almost of the targets of internal use of radioisotopes are the therapy for thyroid diseases (Table 6). The total amount of I-131 used in this country for therapy during one year from July 1986 to June 1987, was 55Ci, and 54.7Ci of them were used as NaI. Patients number treated by sodium radioiodide was 1983. 1472 of them were cases with hyperthyroidism and rest of them were cases with thyroid cancer metastasis.

7. Equipments available in nuclear medicine practice

Equipments available in nuclear medicine department or division consist of conventional scintillation cameras, single photon computed tomographic systems, so called SPECT systems, data processing systems attached to scintillation cameras and so on. In January 1987, 1192 conventional scintillation cameras, 376 SPECT systems and 757 work stations or mini-computers were available in nuclear medicine practice in Japan. And in January 1990, 1152 conventional scintillation cameras, 752 SPECT systems and 1098 work stations or mini-computers were available in Japan. SPECT systems and work stations are increasing in number rapidly.

8.Nuclear medicine speciality in Japan

By 1991, 563 medical doctors have been certificated as a nuclear medicine specialist by the Japanese Society of Nuclear Medicine, and 135 hospitals have been certificated as a training institution for nuclear medicine practice by the Japanese Society of Nuclear Medicine.

Concluding remarks

The recent development of imaging procedures such as X-ray CT, ultrasound and nuclear magnetic resonance technic is remarkable. However,these modalities are used mainly to detect morphological changes. On the contrary, regional tissue function can be studied non-invasively only by using radioisotopic tracers.

In this presentation, the status of general nuclear medicine in Japan was presented.

Legend for figures

Figure 1. Mapping of dopamine D_2 receptors using ^{11}C-N-methyl-spiperone(A) and benzodiazepine receptors using ^{11}C-flumazenil (B)

Figure 2. Variations in the amount of representative radionuclides for in vivo study

Figure 3. The frequency of in-vivo examinations

Figure 4. Numbers of in-vivo examinations per year in a medical college hospital

Table 1. Nuclear Medicine Facilities in Japan

Medical School in Number: 79

PET Facilities with Cyclotron: 19

Equipments in General Nuclear Medicine Practice

	January 1987	January 1990
Conventional Scintillation Camera:	1,192	1,152
SPECT System:	376	752
Work Station for Nuclear Medicine:	757	1,098

Table 2. Number of Nuclear Medicine Facilities in Japan

	1987	1988	1989	1990	1991
Both In Vivo / In Vitro	604	580	562	517	478
In Vivo only	487	530	562	627	672
In Vitro only (Hospital)	113	101	72	61	41
In Vitro only (Private Assay Labo.)	85	85	80	66	62
Total Facilities	1,289	1,296	1,276	1,271	1,253
Total of In Vivo Fac.	1,091	1,110	1,124	1,144	1,150
Total of In Vitro Fac.	802	766	714	644	581

Table 3. Radionuclides for In Vivo study

(MBq)

	1987	1988	1989	1990	1991
^{99}Mo-^{99m}Tc Generator	149,771,375	154,359,375	163,457,675	171,220,275	177,815,525
^{99m}Tc	47,030,811	53,335,352	63,843,759	80,021,195	91,777,316
^{133}Xe	37,555,851	33,087,065	32,101,940	29,082,185	28,556,600
^{67}Ga	15,631,945	16,127,930	16,664,356	17,068,618	17,401,803
^{201}Tl	11,413,871	13,132,965	15,199,600	17,947,368	20,282,882
^{131}I	3,753,650	3,922,185	3,959,032	4,022,760	4,262,075
^{81}Rb-^{81m}Kr Generator	801,050	792,355	813,445	840,640	874,310
^{111}In	385,799	397,232	344,063	331,964	314,944
^{123}I	5,905,940	7,792,200	8,359,361	8,730,275	10,586,107
^{75}Se	22,755	17,279	10,258	6,216	4,421
^{51}Cr	46,916	41,514	36,963	34,632	29,581
^{59}Fe	3,774	3,145	3,117	2,794	2,321
^{57}Co Vitamin B12	25.9	22.2	17.0	17.3	17.0

Table 4. Cold Kits of ^{99m}Tc for In Vivo Study

(Vials)

	1987	1988	1989	1990	1991
Heart,Lung,Brain (HSA,MAA,HM-PAO)	35,856	35,690	46,396	70,925	81,822
Liver, Spleen (Phytate, Tin-colloid)	65,815	61,645	59,504	53,780	47,424
Hepato-Biliary System (HIDA,E-HIDA)	5,655	4,455	2,890	2,250	1,632
Kidney (DTPA, DMSA)	42,769	41,477	40,805	42,316	37,773
Bone (PYP, MDP, HMDP)	145,610	148,813	151,987	150,982	151,581
Others	1,200	0	0	0	0
Total	296,905	292,080	301,582	320,253	320,232

Table 5. Number of Test Tubes for In Vitro Studies

(Test Tubes)

	1987	1988	1989	1990	1991
(1)Pituitary Hormones	7,643,033	7,075,638	6,919,314	6,816,374	7,614,983
(2)Thyroid & Parathyroid Hormones	11,512,680	11,969,740	11,822,367	11,556,434	12,039,029
(3)Pancreas & Gastrointestinal Hormones	5,788,100	5,541,835	5,337,575	5,181,805	5,256,560
(4)Placental Hormones	338,400	274,300	233,800	228,400	227,492
(5)Steroid Hormones	2,604,070	2,874,030	3,038,790	2,939,430	2,159,014
(6)Tumor related substances	23,024,169	25,153,823	24,860,173	20,123,732	20,155,207
(7)Immunoglobulins	5,139,450	5,802,650	7,119,550	7,973,730	7,335,738
(8)Enzymes	2,807,080	3,508,705	3,587,825	2,982,235	3,065,780
(9)Specific antigens & antibodies for virus	9,984,100	9,563,550	8,750,000	7,776,991	8,228,050
(10)Drugs	218,450	214,500	340,550	348,850	319,400
(11)Others	6,441,145	7,919,434	8,294,808	8,886,330	10,070,956
Total	75,500,677	79,898,205	80,304,752	74,814,311	76,472,209

(1) ACTH,GH,FSH,LH,Prolactin,TSH,n-TSH,AVP
(2) T3up,T3RIA,FreeT3,T4RIA,n-T4,FreeT4,Thyroglobulin,PTH,Calcitonin,Thyroglobulin-Ab
(3) Insulin,C-peptide,Glucagon,Gastrin,Secretin
(4) HCG,β-HCG,HPL
(5) Cortisol,Aldosterone,Progesterone,17α-OHP,Testosterone,Free-Testosterone,E2,E3
(6) AFP,CEA,Ferritin,β2-Microglobulin,CA19-9,CA125,CA15-3,SCC,TPA,PA,SP1, POA,SLX,CA72-4,SPan-1,CA130,STN
(7) IgE-RIST,IgE-RAST
(8) Trypsin,PSTI,PAP,Elastase I,Pepsinogen I,NSE,PⅢP,2-5A,TK,Ⅳ-Collagen,PLA;
(9) HBs-Ag,HBs-Ab,HBe-Ag/HBe-Ab,HBc-Ab,HBc-IgMAb,HA-Ab,HA-IgMAb,HDV,HBV-DNA,HCV-Ab
(10) Digoxin,Digitoxin,Cyclosporin
(11) anti-DNA,Renin,β-TG,Myoglobin,PF4,TIBC,UIBC,VB12,C-AMP,Somatomedin-C, Albumin,α I-microglobulin,E2-receptor,Osteocalcin,TBG,TSH-Receptor Ab,CG, Histamin,Metanephrine,Normetanephrine,HPV,HANP,Myosin,Folate,EPO,DNA Prove

Table 6. Internal Use of Unsealed Radioisotopes for Therapy

Period	from July 1986 to June 1987
Facilities	80 Hospitals in Japan

	I-131(NaI)	others
Total Dose in mCi	54657	366
No. of Patients	1983	7
Cases with Hyperthyroid	1472	
Cases with Thyroid Cancer Metastasis	481	
Cases with Other Diseases		12

Fig 1.

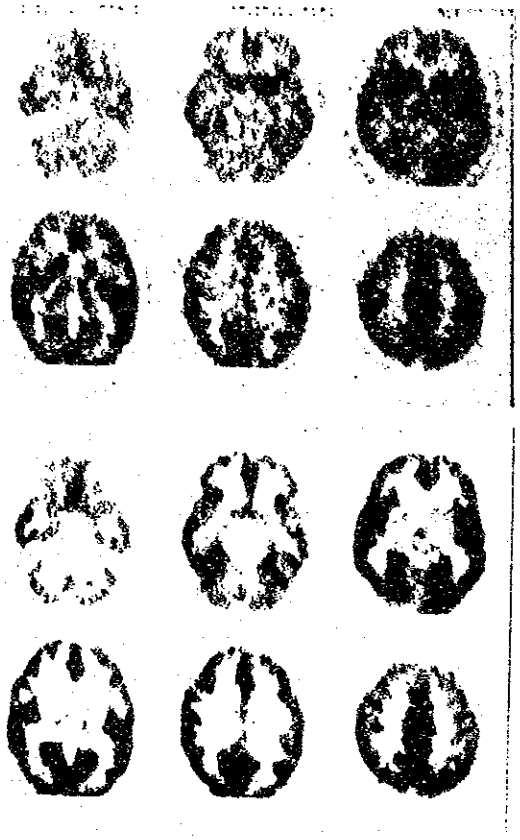

(A)

(B)

Fig 2.

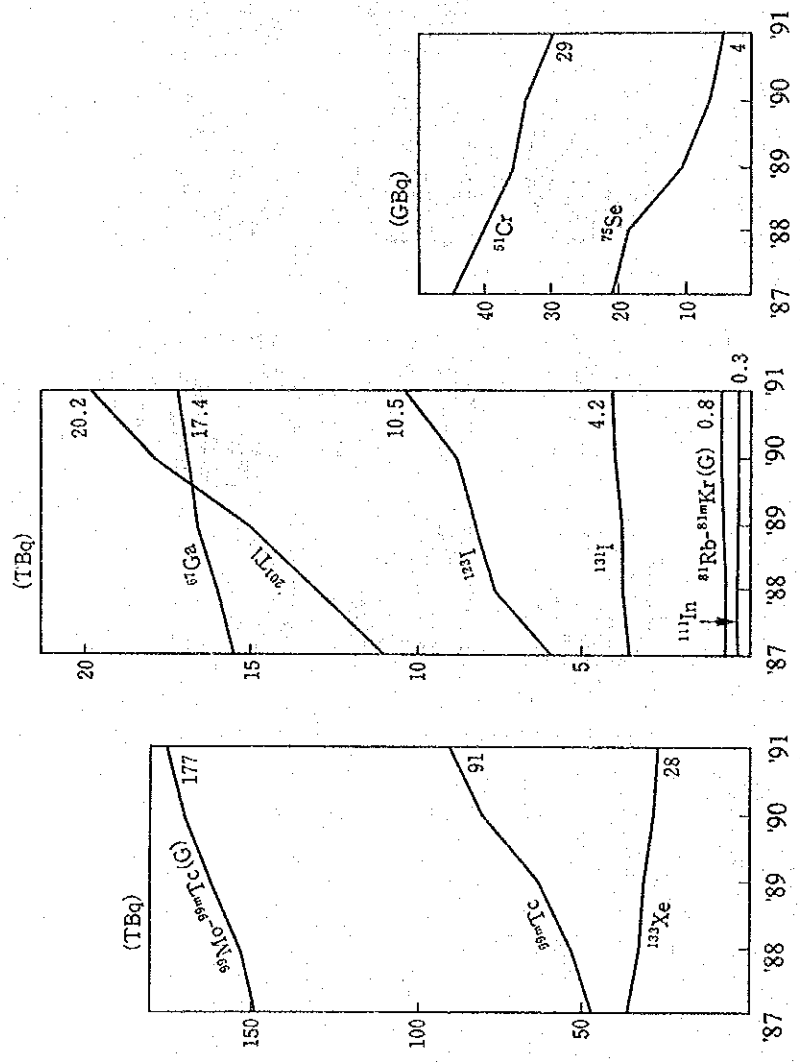
(TBq)
150
100
50
^{99}Mo-^{99m}Tc(G)
177
^{99m}Tc
91
^{133}Xe
28
'87
'88
'89
'90
'91
(TBq)
20
15
10
5
^{67}Ga
20.2
^{201}Tl
17.4
^{123}I
10.5
^{131}I
4.2
^{111}In
^{81}Rb-^{81m}Kr(G)
0.8
0.3
(GBq)
40
30
20
10
^{51}Cr
29
^{75}Se
4

Fig. 3.

Frequency of In-Vivo Examinations(1982)

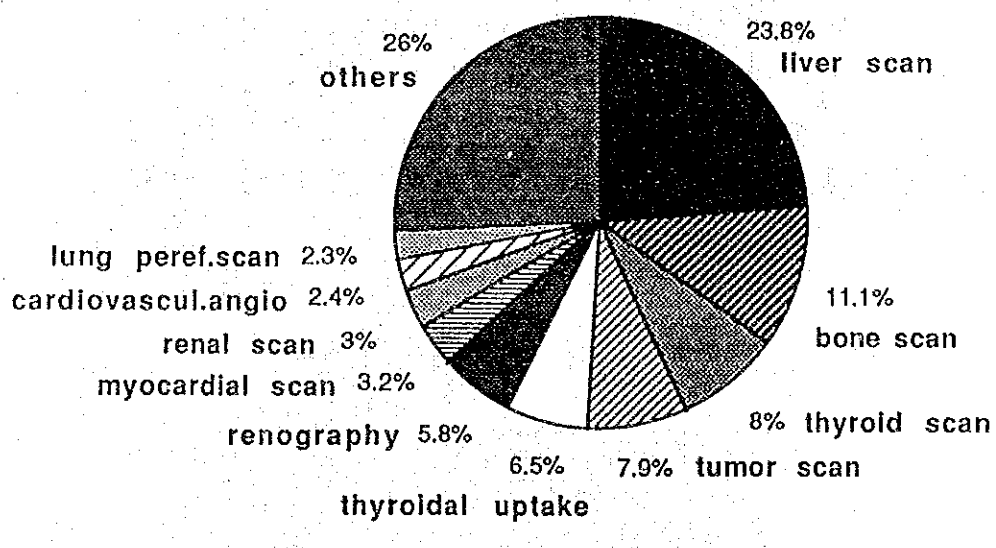

Frequency of In-Vivo Examinations(1987)

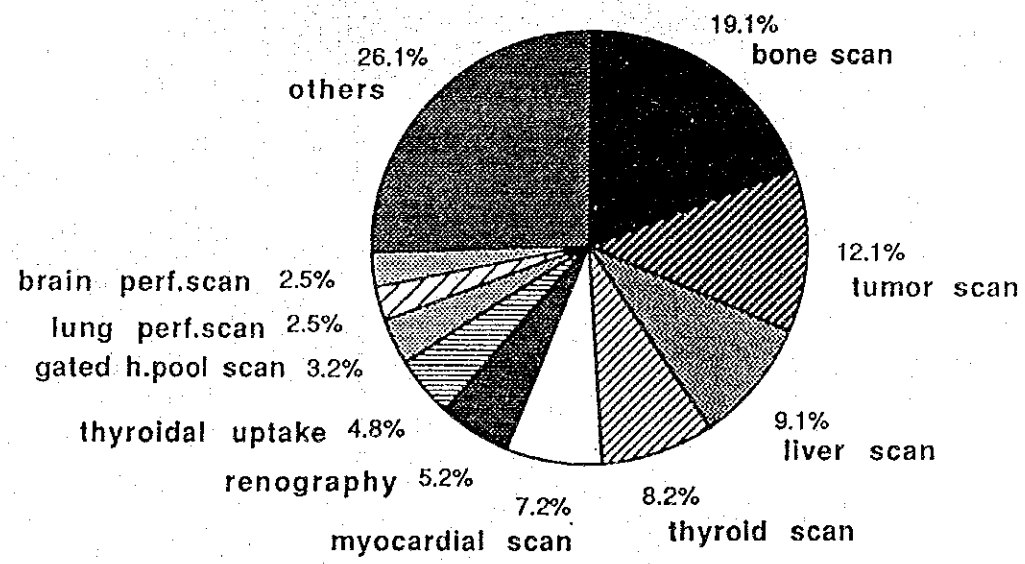

Numer of In Vivo Examinations
Tokyo Women's Medical College Hospital
6619 cases ,April,1989-March,1990

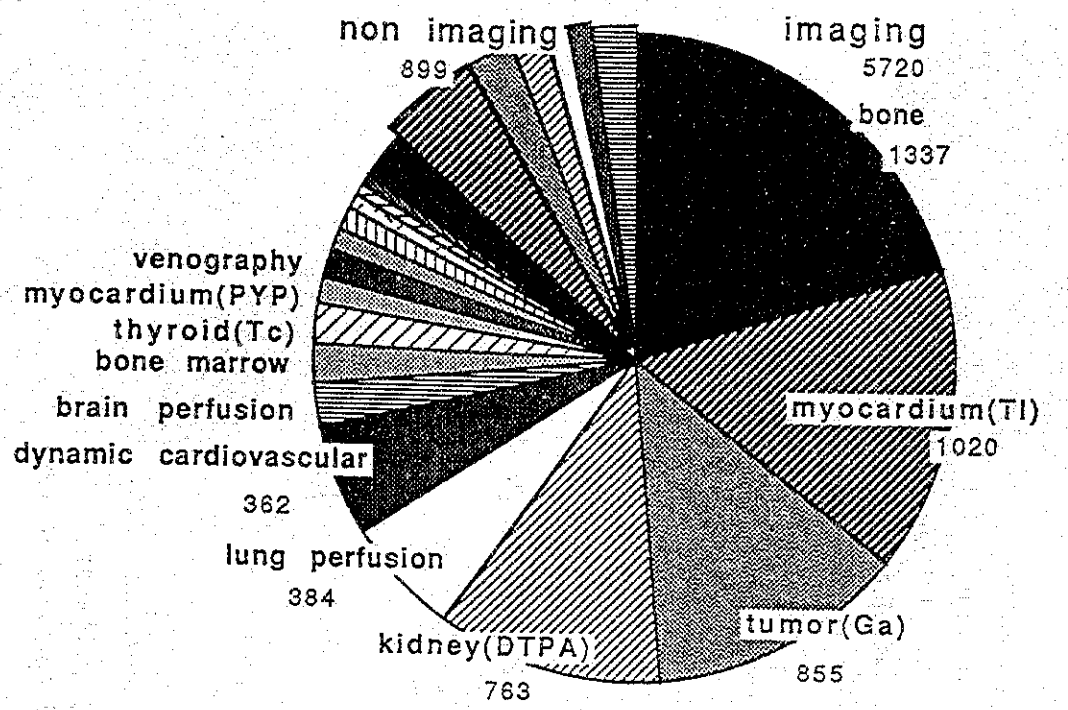

Fig 4

NUCLEAR MEDICINE OF THE BRAIN
: Neuro-nuclear Medicine

Fumio Shishido, M.D., Kazuo Uemura, M.D.*

Division of Clinical Research
National Institute of Radiological Sciences,
Chiba, 263 Japan
*Research Institute for Brain & Blood Vessels-Akita,
Akita, 010, Japan

Diagnosis of the central nervous system (CNS) is one of the most advanced fields of nuclear medicine. Even though classical brain scintigraphy was affected by the rapid penetration of X-ray computed tomography, the further progress of neuronuclear medicine has been remarkable, especially in the field of functional brain study using emission computed tomography. Nuclear medicine of the brain can be divided into three categories:

1. Imaging of intracranial focal lesions
2. Imaging of cerebrospinal fluid circulation
3. Regional functional study of the brain

1. IMAGING OF INTRACRANIAL FORCAL LESIONS

: Brain scanning and radionuclide cerebral angiography

Before CT-era, brain scanning was widely performed as a routine means of noninvasive diagnosis of intracranial lesions. With its superior spatial resolution, X-ray CT has advantages for the pathologic and morphologic diagnosis of brain diseases, however, conventional X-ray CT methods hardly provide us with information as to regional brain functions. When we perform a brain scan, it usually is preceded by radionuclide cerebral angiography. radionuclide angiography gives a rough information regarding the cerebral blood vessels and qualitative information concerning regional cerebral perfusion, thus covering the drawbacks of the X-ray CT image.

(1) Method

^{99m}Tc-pertechnetate or ^{99m}Tc-DTPA are used for brain scanning and for radionuclide cerebral angiography. Thirty minutes before ^{99m}Tc-pertechnetate administration, 0.5 g of perchlorate is administered orally to prevent the selective

accumulation of ^{99m}Tc-pertechnetate in the choroid plexus. Radionuclide(RN) cerebral angiography is taken with the patient lying on his back. A bolus of 15-20 mCi pertechnetate is injected. Bolus injection of the ^{99m}Tc is performed by the saline flushing method. Depend on the location of the brain lesion, several projections, anterior, posterior, vertex, etc., are selected.

Radionuclide cerebral angiography is followed by a conventional static brain scan. An early scan taken immediately after the RN angiography by a delayed scan 2-4 hours later is recommended. The early scan is suitable for the detection of activity in the cerebral blood vessels and the delayed scan is sensitive to the radioactivity accumulated in a tumor and an infarction of the brain. The addition of a vertex view is useful. Application of single photon emission computed tomography (SPECT) gives increased detectability and reveals the spatial distribution of lesions in detail.

(2)Scan Reading

Normal brain tissue is protected by the blood-brain barrier and remains a low-count area of the brain scan, surrounded by the peripheral band with high count. Superficial blood pools such as the superior sagittal sinus and the transverse and sigmoid sinuses reveals high-count areas. Thick muscles such as the temporal muscle also increase background. The cerebellum is separated from the cerebral region by the high-count band of the transverse sinus.

Brain lesions are revealed as high-count areas. This is due to the increased permeability of capillaries and the abnormal increase in vessel volume of the brain lesion. Abnormal high-count lesions are caused by intracranial lesion, skull lesion, and even by the scalp.

About eighty percent of brain tumors can be visualized by the radionuclide brain scan. Meningioma, malignant glioma, glioblastoma, and metastatic brain tumor are most

significantly visualized by this method. However, low grade gliomas have no abnormal uptake of ^{99m}Tc-DTPA.

The most remarkable positive scan is observed 3-4 weeks after onset in cerebral infarction and intracerebral hematoma, However, they usually remain negative in the periods immediately after and several months after the episode. Cerebrovascular diseases (intracerebral hemorrhage and cerebral infarction) are characterized by the fact that

(a) accumulation of radionuclide shows remarkable changes according the time after onset and

(b) the location of the lesion in cerebral infarction corresponds to the distribution of the cerebral arterial blood supply. Hypertensive intracerebral hematoma usually produces a faint positive scan, which is revealed as a ringlike abnormal uptake around the hematoma by emission CT.

The brain abscess becomes positive at the stage of encephalitis and increases its density as the abscess forms. Early detectability of brain abscess by brain scan is still highly regarded.

Radionuclide cerebral angiography provides us with information on vessel images of the main trunks of cerebral perfusion. In a normal subjects, activity indicates simultaneous bilaterally and equal appearance of arterial phase followed by intermediate phase and venous phase. Pathologic findings may be summarized as follows:

(i) Decreased regional perfusion: This lesion is expressed by the regional low count and prolonged circulation time. These abnormalities are caused by occlusion or severe stenosis of the cerebral artery (cerebral infarction), transient ischemic attack or by compressions with mass lesions (hematoma, avascular tumor, chronic subdural hematoma, etc.).

(ii) Increased regional perfusion: This lesion is either due to an increased pool of vessels or increased regional blood flow (arteriovenous fistula, vascular tumor, luxury perfusion, and epileptic seizure). Reading of RN angiography combined with

conventional brain scan helps to increase of the sensitivity and specificity of the diagnosis of brain lesions. Even if an major cerebral artery is occluded, CT scan is negative at the early stage of onset within 5 hours. However, radionuclide cerebral angiography almost always detects the occlusion of the arterial main trunk, and the grade of collateral circulation will be simultaneously estimated.

2. IMAGING OF CEREBROSPINAL FLUID CIRCULATION: Radionuclide Cisternography

Radionuclide cisternography is imaging of cerebrospinal fluid space by the intrathecal injection of a radiopharmaceutical that does not hinder physiologic cerebrospinal fluid (CSF) circulation.

(1) Method

0.5-1.0 mCi of ^{111}In-DTPA is intrathecally injected at the level of the lumbar vertebrae. Keeping the patient still by placing him on this abdomen for the initial few hours to prevent leakage of the tracer through the punctured hole, four projections of the brain: anterior, posterior, right lateral, and left lateral, are imaged by a gamma camera or SPECT at 4, 24, and 48 hours after the injection. Quantitative analysis of the radionuclide inflow and outflow from the intracranial space also is carried out by consecutively recording counts.

(2) Scan Reading

Cerebrospinal fluid, produced mainly by the choroidal plexus in the lateral, third, and fourth ventricles, flows out through the foramina Lushika and Magendie into the subarachnoidal space, reaches cerebral surface via the tentorial notch, and is reabsorbed, principally into the blood, by arachnoidal villi distributed along the superior sagittal sinus. Part of the CSF flows down from the basal cistern into the spinal canal and flows

back intracranially. The CSF can be reabsorbed outside of arachnoidal villi, and this mechanism becomes remarkable in diseased conditions due to abnormal CSF flow. RN cisternography is a valuable means of detecting such an abnormality.

Normal RN cisternography visualizes the Sylvian fissure symmetrically 3-6 hours after intrathecal injection, and accumulates in the parasagittal region for reabsorption at 24-48 hours after injection. The ventricle is not visualized.

Abnormal findings of RN cisternography are ventricular reflux, subarachnoid regional block, regional retention of radionuclide and extrathecal leakage. Ventricular reflux of radionuclide is evaluated as an important sign of normal pressure hydrocephalus (NPH). Screening of normal pressure hydrocephalus from senile dementia is an important problem in geriatric practice. Marked ventricular reflux is seen from an early stage of injection and persists for more than 24 hours. Little activity is seen in the subarachnoid space above the tentorium cerebelli. When more activity, accompanied by delayed circulation and ventricular retention of radionuclide is seen above the tentorium cerebelli, diagnosis may be NPH or brain atrophy. Delayed circulation of CSF and transient ventricular reflux may be caused by brain atrophy.

Regional blockage of the subarachnoid space and regional radionuclide retention are caused by compression of a mass lesion, regional blockage of the subarachnoid space, and arachnoid cyst, etc. Arachnoid cyst in particular shows significant inflow of radionuclide into the cyst, becoming even clearer after 24 hours, indicating the reabsorption of CSF at the lesion.

3. REGIONAL FUNCTIONAL STUDY OF THE BRAIN

Currently, only nuclear medicine enables in vivo assessment of regional cerebral blood flow (rCBF) and metabolism. Recent progress in emission computed tomography (emission CT), especially in positron emission tomography (PET) has made possible measurements not only of rCBF but also of the energy metabolism and other biochemical

processes of the brain. These study would contribute to clarify the physiological and pathophysiological process of the brain.

(1) Two Dimensional rCBF Study Using the ^{133}Xe Clearance Method

This is the most common method which measures the cerebral transit process of ^{133}Xe introduced into the brain tissue. The measurement is made by multiple scintillation detectors or a gamma camera. The ^{133}Xe clearance curve from the brain is usually analyzed by three different methods: two-compartment analysis, height-over-area method and initial-slope method.

With the ^{133}Xe intracarotid injection method, administration of ^{133}Xe saline solution into the internal carotid artery is usually performed following cerebral angiography. Since a sufficient amount of ^{133}Xe can be introduced by this method, the gamma camera measurement provide an image of rCBF.

Different from this traumatic procedure, a nontraumatic ^{133}Xe inhalation or intravenous injection method also has been adopted. With this method, recirculation and extracranial contamination of ^{133}Xe are also counted simultaneously but must be sufficiently corrected for the calculation of cerebral blood flow. The advantages of this method are its noninvasiveness and simultaneous measurement of regional blood flow of the whole brain. At present, factories provide the computer controled devices which are applicable to rCBF measurement with both the ^{133}Xe intracarotid injection and inhalation techniques.

(2) Three Dimensional rCBF Mapping Using a Single Photon Emission Computed Tomography (SPECT)

The two dimensional rCBF study using the ^{133}Xe clearance has following difficulties.

(i) Because of superimposition of tissue layers in each detector field, spatial resolution of the study is severely limited, and information from a deep seated lesion is spoiled.

(ii) An area with severe ischemia, even if lying directly underneath a detector, will ignored due to proportionally decreased input of ^{133}Xe into the lesion. -i.e. "Look Through" phenomenon.

In order to overcome these difficulties, the three dimensional rCBF study using a emission CT is useful. The author group have developed a series of emission tomograph; named HEADTOME. At present, we use HEADTOME-II for SPECT. The method measuring rCBF using SPECT can be divided to the following groups;

(i) the ^{133}Xe clearance method,

(ii) the tracer trapping method with N-isopropyl-p-^{123}I-iodoamphetamine (^{123}I-IMP), ^{99m}Tc-hexamethyl-propyleneamineoxime (^{99m}Tc-HM-PAO) and ^{99m}Tc-ethyl cysteinate dimer (^{99m}Tc-ECD).

In stroke patients, decrease of rCBF is more extensive than had been suspected on the basis of X-ray CT. This dissociation of the findings between the finding of the tomographic rCBF study and the X-ray CT may be resulted from the following factors:

a) the perfusion pressure of the collateral pathway developed in the area outside of the low density brain will be lower than the lower limit of the autoregulatatory range, and

b) decreased excitation of remote neurons connected from the necrotic (low density) brain tissue, i.e. diaschisis.

(3) Functional Brain Study Using Positron Emission Computed Tomography

Positron emission computed tomography (PET) is the most excellent means for in-vivo quantitative measurement of regional physiological variables in the human brain. rCBF is one of principal variables of the brain tissue, but, in an ischemic cerebral lesion accompanying with tissue acidosis, it is strongly influenced by a tissue perfusion

pressure, and in some time does not correctly reveal the grade of tissue damage with ischemia. Using PET and tracer labeled with positron emitting radionuclides such as ^{11}C, ^{13}N, ^{15}O and ^{18}F, regional pathophysiology of cerebral ischemia and other cerebral disease can be evaluated in correlation with rCBF and energy metabolism.

The mapping of regional glucose consumption rate (CMRGlc) can be measured by an intravenous injection of ^{18}F-fluorodeoxyglucose (^{18}FDG) enters the brain tissues is phosphorylated by brain hexokinese, and the metabolic product; ^{18}FDG-6-PO_4 remains fixed within the tissue. Regional CMRGlc is given by measuring ^{18}FDG in the brain tissue and concentration of ^{18}FDG and of plasma glucose.

Regional oxygen consumption rate ($CMRO_2$) can be measured by continuous inhalation of $C^{15}O_2$ and $^{15}O_2$ using the ^{15}O steady state model. Inhalled $C^{15}O_2$ is transferred to $H_2{}^{15}O$ in the lung and enters brain tissue as a function of rCBF. When inhaled subsequently as $^{15}O_2$, the tracer is bound to hemoglobin, enters the brain as oxyhemoglobin, is extraced as a consequence of regional oxygen metabolism transferring to metabolic $H_2{}^{15}O$. PET study during equilibrium breathing of $C^{15}O_2$ gives rCBF. The ratio of brain tissue activities measured by PET during inhalation of $^{15}O_2$ and $C^{15}O_2$, respectively, gives the oxygen extraction fraction (OEF) which means the ratio of value of oxygen content. The $CMRO_2$ is calculated by the product of the OEF, CBF and arterial oxygen content.

The changes of these variables after stroke and those correlation with the morphological changes on the X-ray CT are shown. Flow/metabolism uncoupling in the acute phase, i.e. the "misery perfusion" and "luxury perfusion" is also clearly demonstrated.

A remarkable correlation between glucose metabolic rate and histological grade of the gliomas was demonstrated with PET and ^{18}FDG. The most consisted finding is hypermetabolism in malignant gliomas. As described above, positron CT studies are very excellent, but are too expensive for general use. Following the remarkable success of the

positron emission tomography, this approach shall be extended to the more economical SPECT study using tracers labeled by ^{123}I, ^{99m}Tc, ^{133}Xe and so on.

Functional Brain Study

1. Emission Computed Tomography(ECT)

    Single Photon Emission Computed Tomography (SPECT)

    Positron Emission Tomography (PET)

2. SPECT Device

    Rotating single-head(or dual-head) gamma camera system

    Triangle gamma camera(triple-detector) system

    Rectangle gamma camera system

    Circular detector system

3. PET Device

    Multislice PET

    TOF-PET

4. Tracers

Parameters	SPECT tracer	PET tracer
CBF	^{133}Xe	$C^{15}O_2$
	^{123}IMP	$H_2{}^{15}O$
	99mTc-HM-PAO	
	99mTc-ECD	
energy metabolism		$^{15}O_2$
		^{18}FDG, ^{11}CDG
amino acid metabolism	^{123}I-iodo-methyl-tyrosine	^{11}C-methionine
		^{11}C-tyrosine
nucleotide metabolism		^{18}F-dUr
neuroreceptor		
acetylcholine	^{123}I-QNB	^{11}C-MQNB
	^{123}I-dexetimide	^{11}C-TRB
		^{18}F-DPET, ^{11}C-DPET
		^{11}C-nicotine
beta1(noradrenaline)	^{123}I-prenalterol	^{11}C-CGP 12177
beta2(noradrenaline)		^{11}C-carazolol
		^{18}F-FAcarazolol
		^{18}F-FAPIN
D1(dopamine)	^{123}I-SCH 23982	^{11}C-SCH 23390

	^{123}I-FISCH	^{11}C-SCH 39166
	^{123}I-TISCH	
D2(dopamine)	^{123}I-IBZM	^{11}C-IBZM
	^{123}I-NCQ 298	^{18}F-NCQ115
	^{123}I-epidepride	^{11}C-raclopride
	^{123}I-2-spiperone	^{11}C-NMspiperone
	^{123}I-ILIS	^{18}F-NFBspiperone
	^{123}I-IBF	^{11}C-NMbenperidol
	^{123}I-IMD	^{11}C-YM 09151-2
	^{123}I-haloperidol	^{76}Br-spiperone
		^{18}F-IBZM
		^{18}F-FABZM
5-HT2(serotonine)	^{123}I-2-ketanserin	^{76}Br-2-ketanserin
5-HT3/1A(serotonine)		^{11}C-MDL 72222
H1(histamine)		^{11}C-pyrilamine
H2(histamine)		^{11}C-ranitidine
CBZ(diazepam)	^{123}I-iomazenil	^{11}C-flumazenil
	^{123}I-2'-IDZ	^{11}C-NMDZ
	^{123}I-G-018	^{18}F-FERO, ^{18}F-FPRO
		^{11}C-alprazolam
PBZ(diazepam)		^{11}C-PK 11195
		^{18}F-PK 14105
NMDA(glutamate)		^{18}F-13MMK 801
Delta,Kappa,Mu(opiate)		^{11}C-diprenorphine
		^{18}F-NPdiprenorphine
		^{11}C-cyclofoxy
Mu(opiate)		^{11}C-carfentanyl

		^{11}C-ohmefentanyl
		^{11}C-buprenorphine
		^{11}C-MPAG
Sigma(opiate)	^{123}I-PIPAG	
	^{123}I-MIPAG	
Somatostatin	^{123}I-Tyr-3-octreotide	
CCK(cholecystokinin)		^{11}C-MK 329

5. Cerebrovascular Disorders

(1) Tracer

CBF & energy metabolism

(2) application

Cerebral ischemia

misery perfusion

luxury perfusion

coupled perfusion

Acute & chronic ischemia

detection of viable tissue : emergent embolectomy or revascularization, thrombolysis, or anticoaglation

6. Brain Tumor

(1) Tracer

glucose metabolism ^{18}FDG

amino acid metabolism and transport ^{11}C-methionine, ^{123}IMT

(2) application

predicting degree of tumor malignancy(prognostic values)

radiation necrosis

7. Dementia

(1) Tracer

CBF & energy metabolism

(2) application

Alzheimer disease

temporo-parietal hypometabolism

Vascular dementia

mainly frontal lobe

Pick's disease

fronto-temporal hypometabolism

Preserved in the primary visual and sensorimotor cortices, basal ganglia, and cerebellum

8. Epilepsy

(1) Tracer

CBF & energy metabolism

(2) application

detection of seizure foci

interictal : hypometabolism(& hypoperfusion)

ictal : hypermetabolism(& hyperperfusion)

9. Head Trauma

(1) Tracer

CBF & energy metabolism

(2) application

good correlation between the severity of head trauma(the Glasgow Coma Score) and the degree of whole-brain hypometabolism

10. Other diseases

(1)Spinocerebellar degeneration

(2)Herpes simplex encephalitis

(3)Creutzhelt Jacob disease

[Normal]

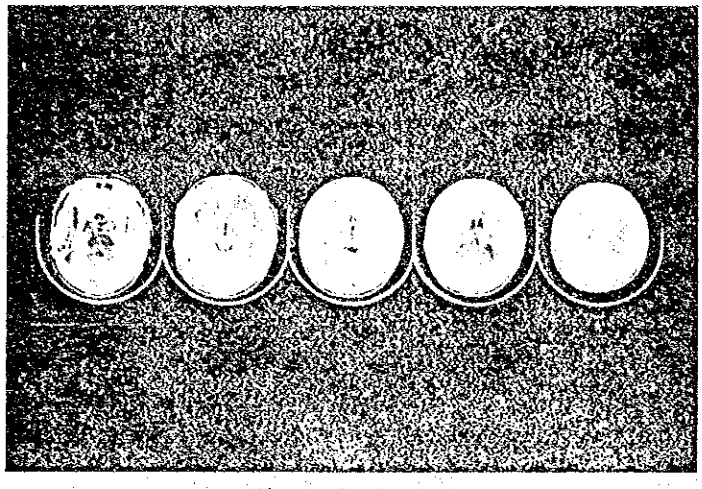

Fig 1. CT images

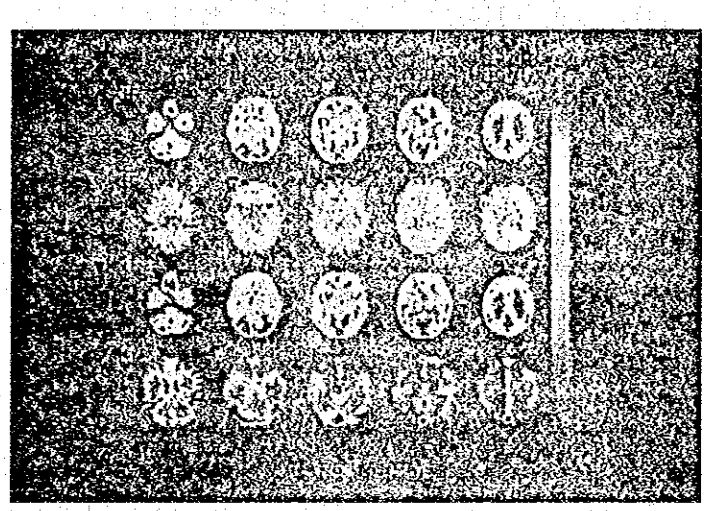

Fig 2. Cerebral blood flow and oxygen metabolism measured by ^{15}O steady-state method ($^{15}O_2$, $C^{15}O_2$, $C^{15}O$)

CBF: cerebral blood flow,
OEF: oxygen extraction fraction,
$CMRO_2$: cerebral metabolic rate of oxygen
CBV: cerebral blood volume

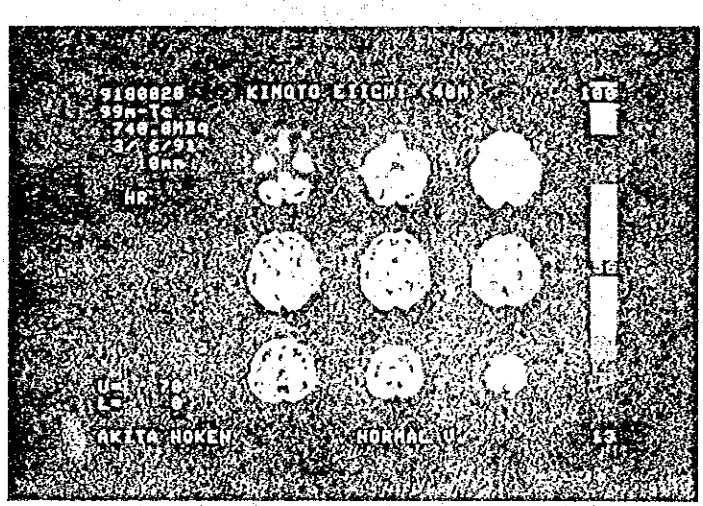

Fig 3. SPECT images using ^{99m}Tc-HM-PAO

[Cerebrovascular disease]

Case 1 Temporal pathophysiological sequence of stroke(8 hrs, 7 days, 29days after onset).

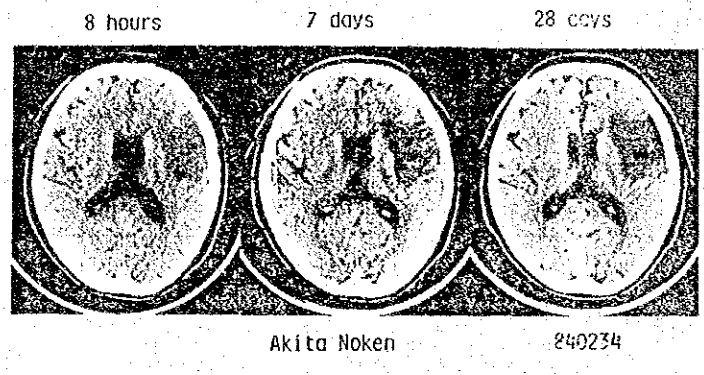

Fig 4 X-ray CT images

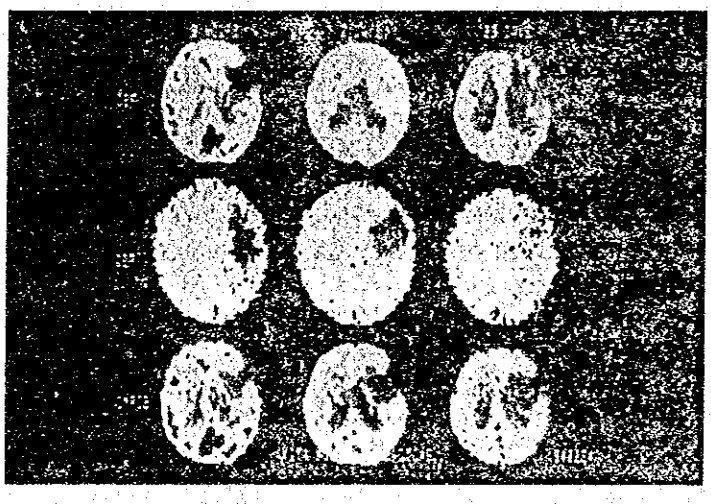

Fig 5 PET(CBF, OEF, $CMRO_2$). The images of rCBF, rOEF, and $rCMRO_2$ studied by the ^{15}O steady state method in a patient with acute cerebral infarction.

Case 2 Acute cerebral ischemia

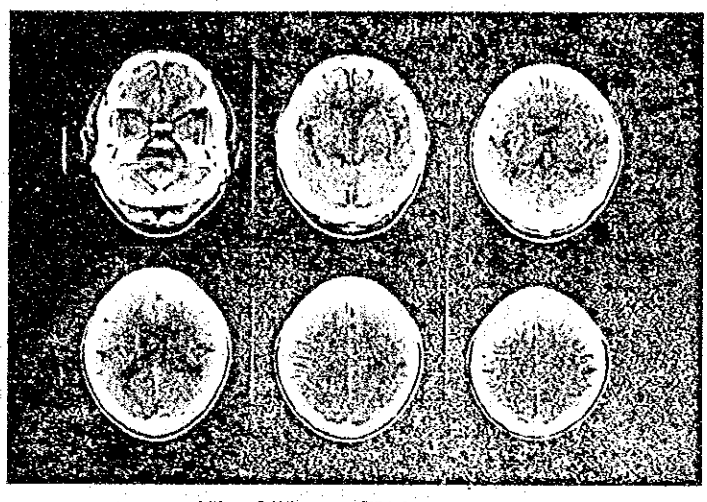

Fig 6 X-ray CT images

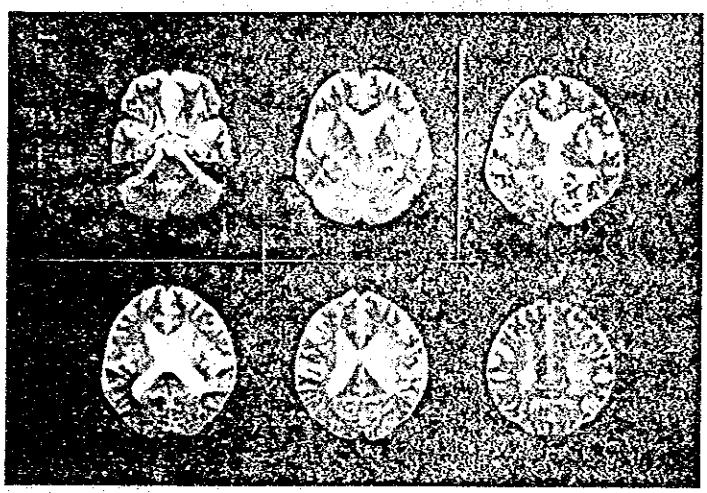

Fig 7 MRI images

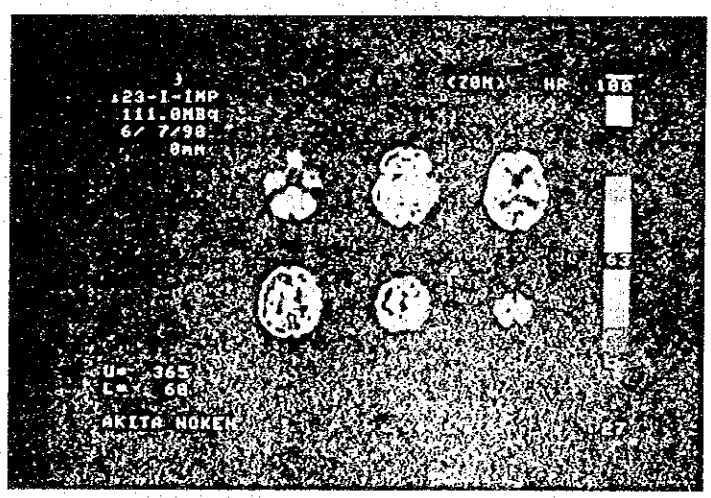

Fig 8 SPECT images using ^{123}IMP

Fig 9 Angiography

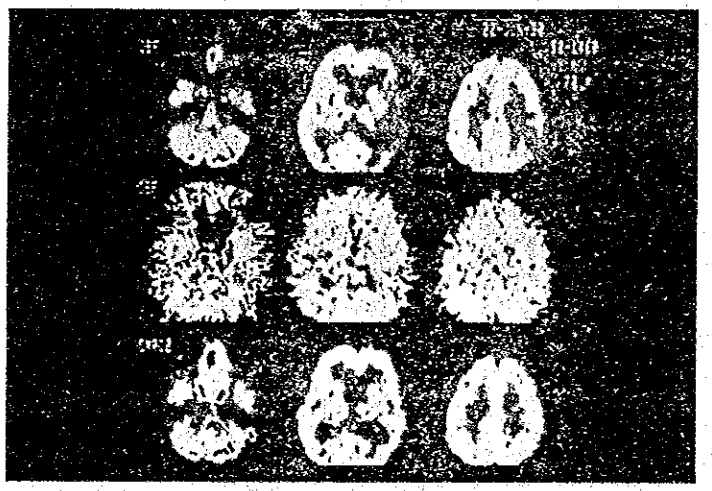

Fig 10 PET images (CBF, OEF, $CMRO_2$)

This patient suddenly showed dementia due to occlusion of right middle cerebral artery.

Case 3. Right internal carotid artery occlusion. Before and after bypass surgery.

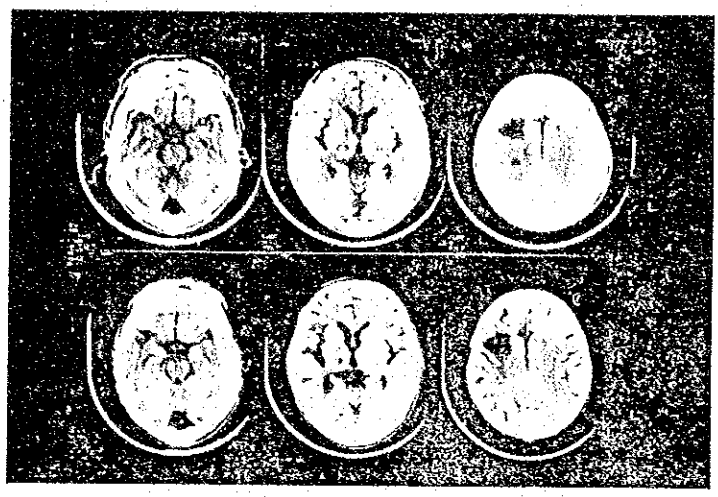

Fig 11 X-ray CT images

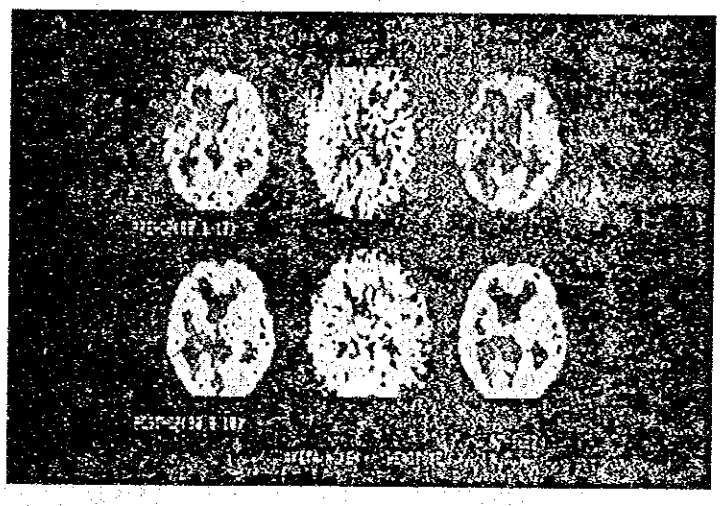

Fig 12 PET images (CBF, OEF, $CMRO_2$)

Case 4 Acute cerebral ischemia

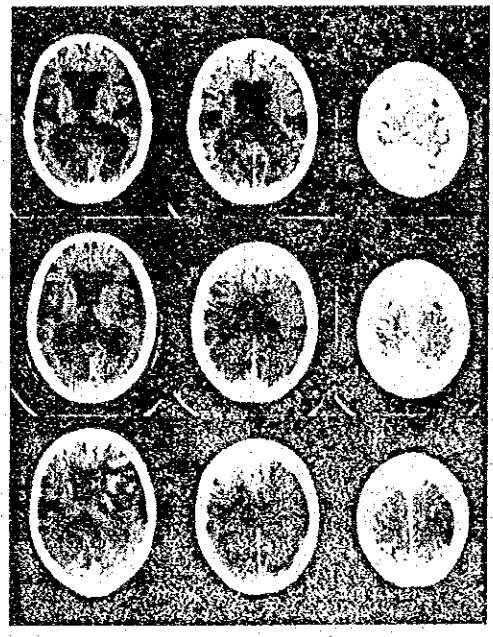

Fig 13 X-ray CT images

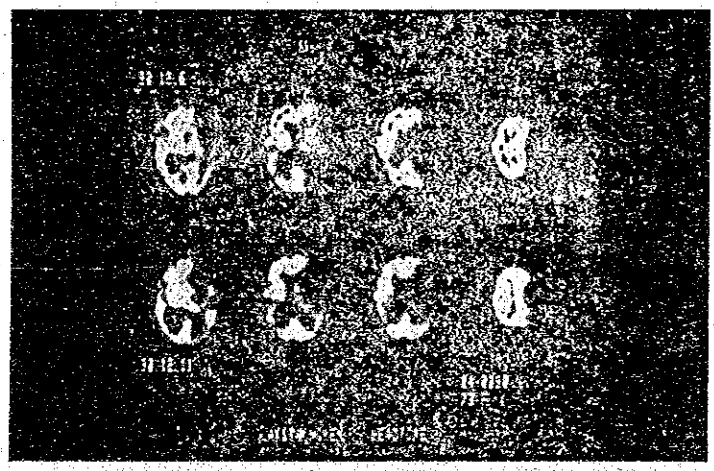

Fig 14 SPECT images using ^{99m}Tc-HM-PAO(before and after embolytic therapy)

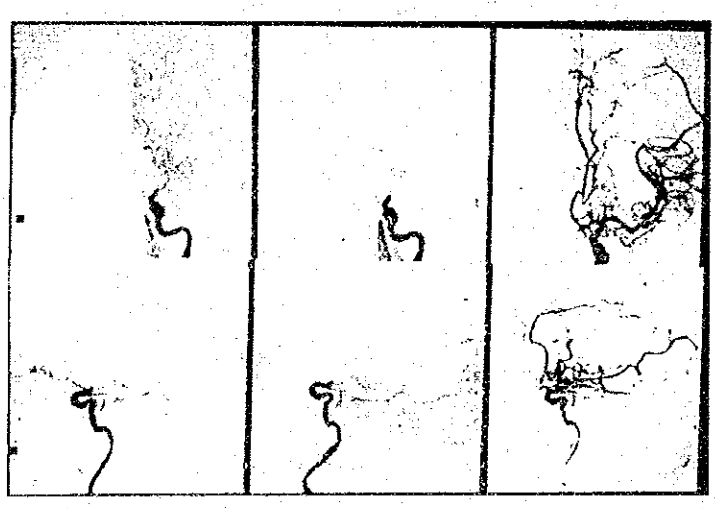

Fig 15 Angiography

Case 5 Acute cerebral ischemia

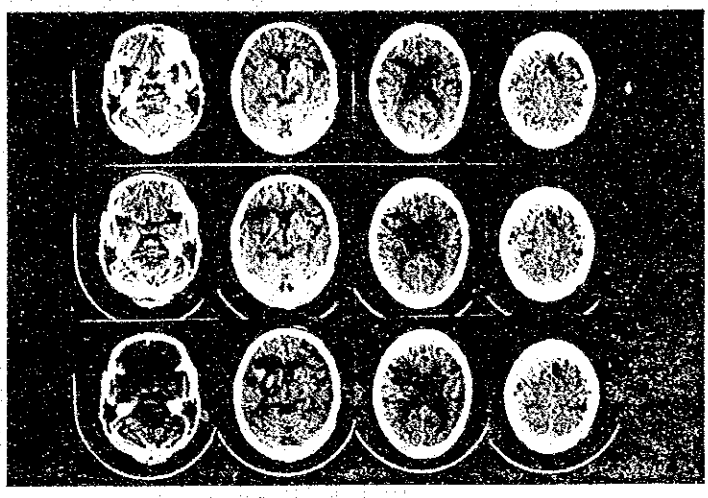

Fig 16 X-ray CT images

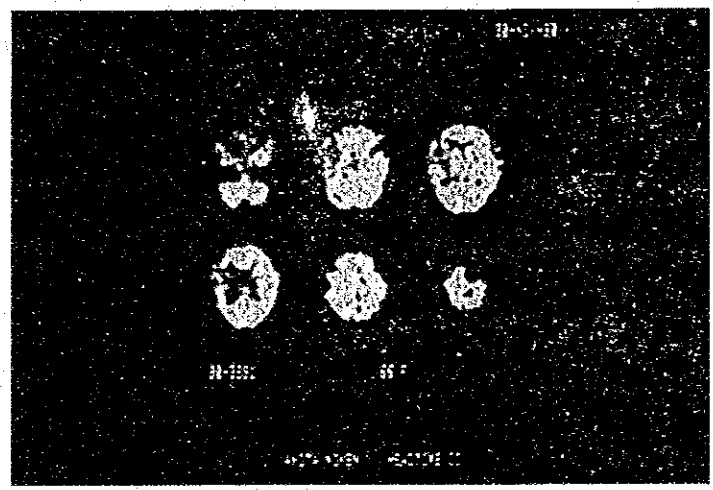

Fig 17 SPECT images using ^{99m}Tc-HM-PAO

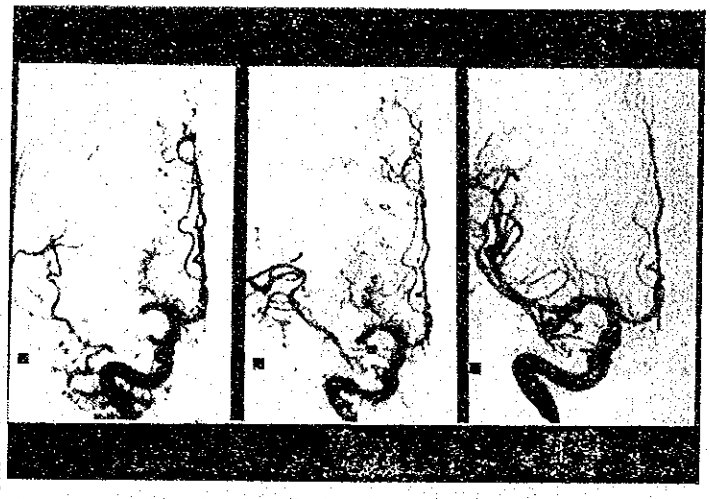

Fig 18 Angiography

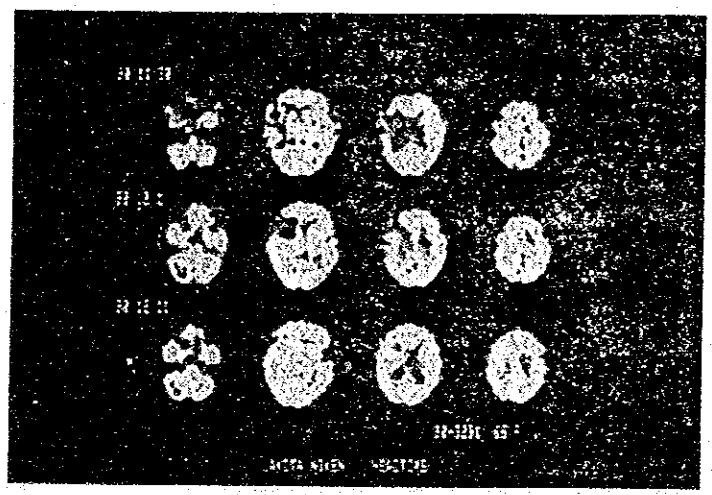

Fig 19 Follow-up study after embolectomy. SPECT images using ^{99m}Tc-HM-PAO

Case 6 Cerebral infarction(crossed cerebellar diaschisis)

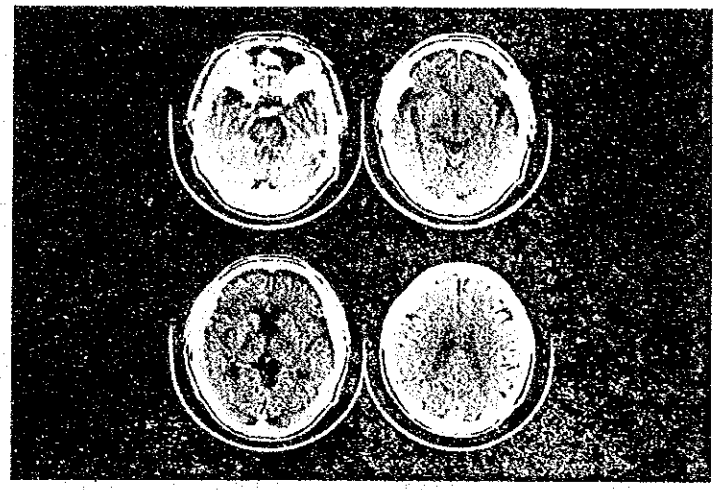

Fig 20 X-ray CT images

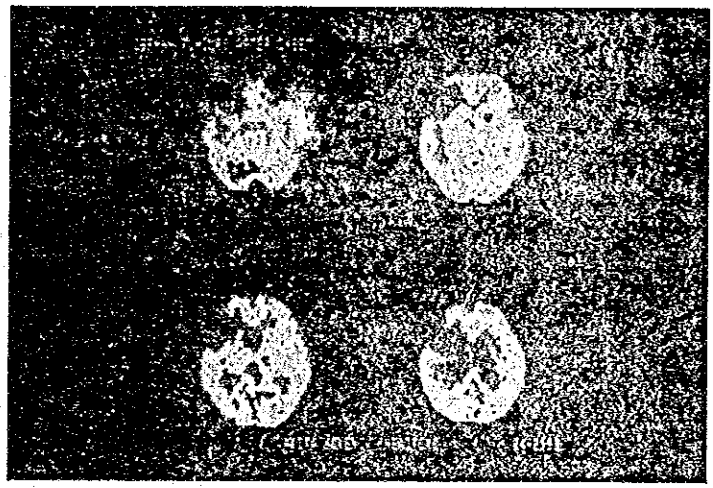

Fig 21 PET images (CBF)

[Brain Tumor]

Case 7 Low grade glioma

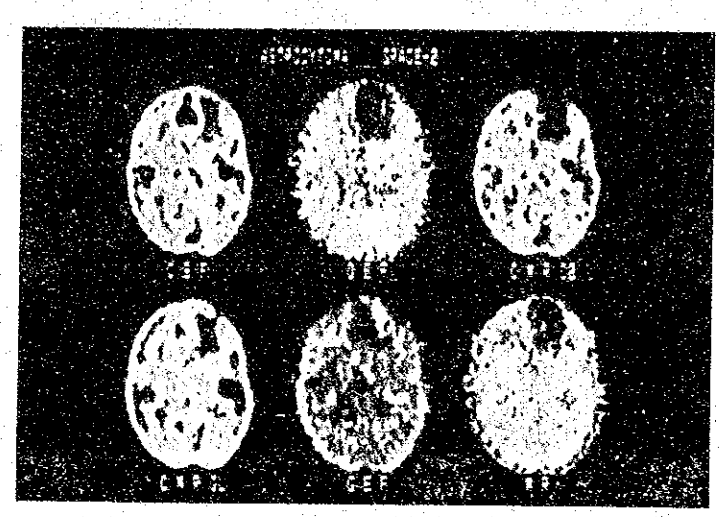

Fig 22 PET images(CBF, OEF, $CMRO_2$, CMRGlc, GEF, MR)

Case 8 High grade glioma

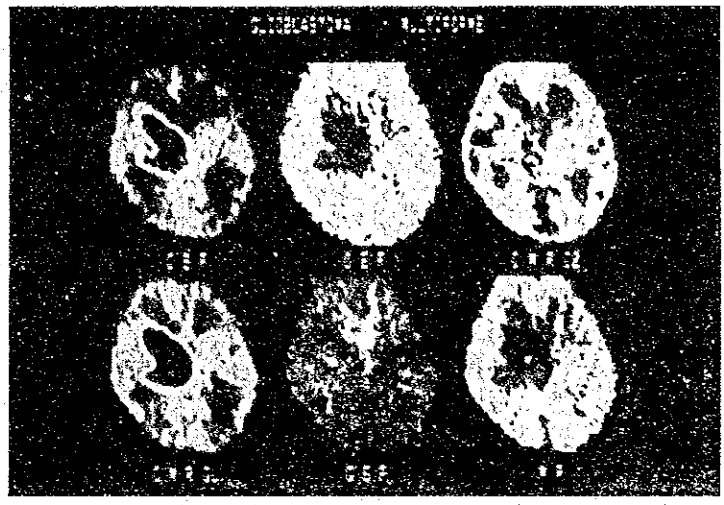

Fig 23 PET images(CBF, OEF, $CMRO_2$, CMRGlc, GEF, MR)

Case 9 Recurrence

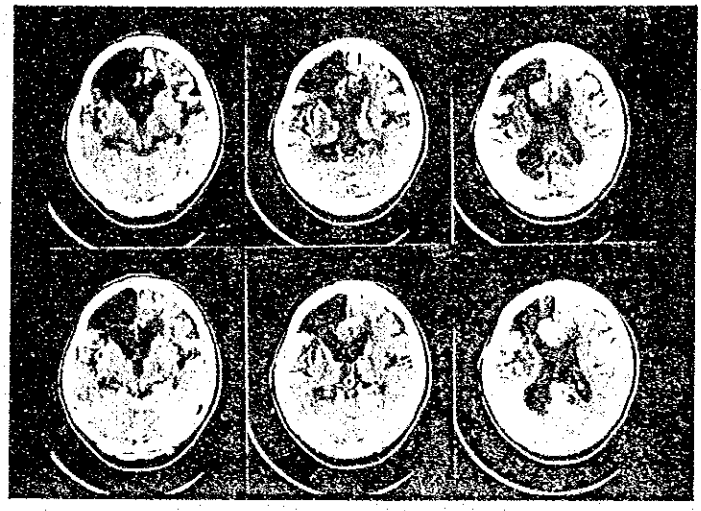

Fig 24 X-ray CT images

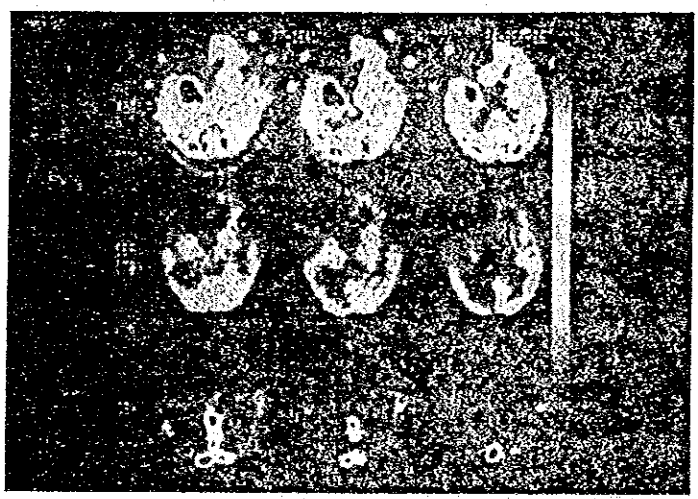

Fig 25 PET images(11C-methionine, CBF, CBV)

Case 10 Radiation necrosis

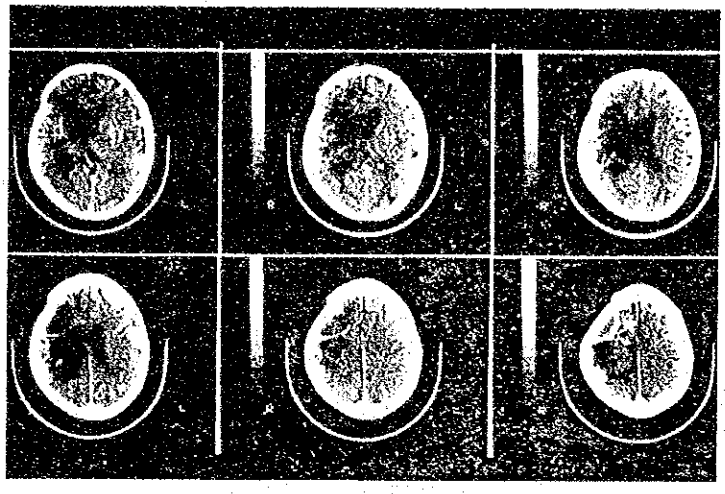

Fig 26 X-ray CT images

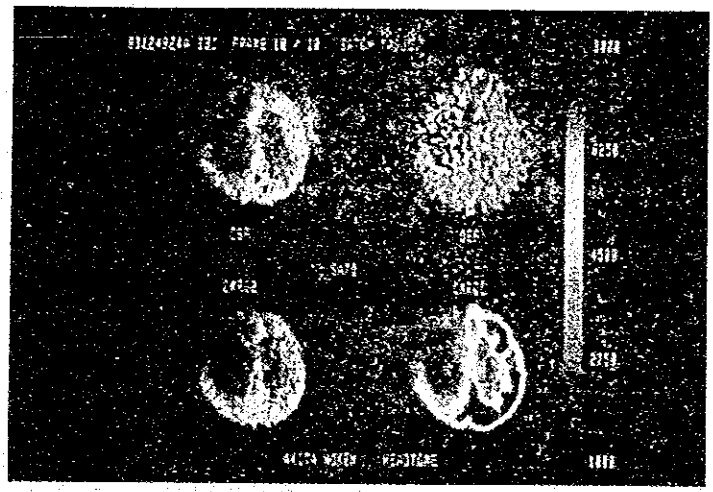

Fig 27 PET images(CBF, OEF, $CMRO_2$, CMRGlc)

[Dementia]

Case 11 Alzheimer disease

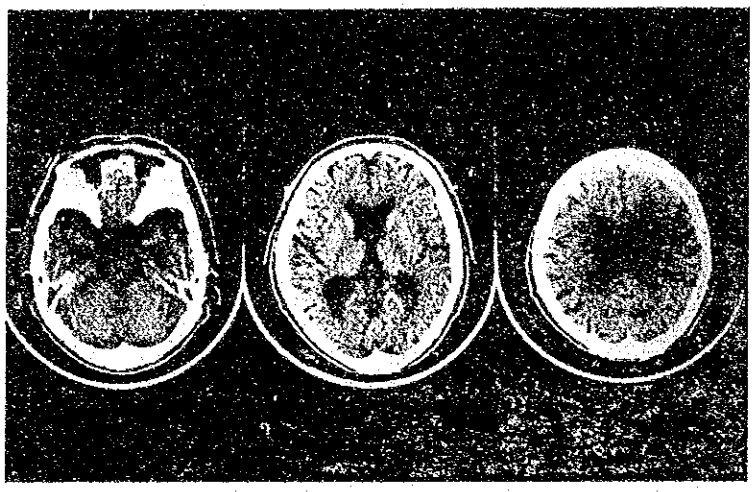

Fig 28 X-ray CT images

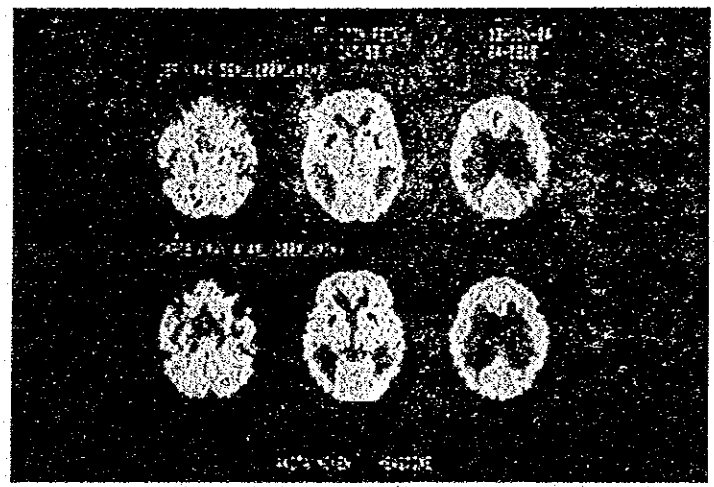

Fig 29 PET images(CBF, $CMRO_2$)

Case 12 Vascular dementia

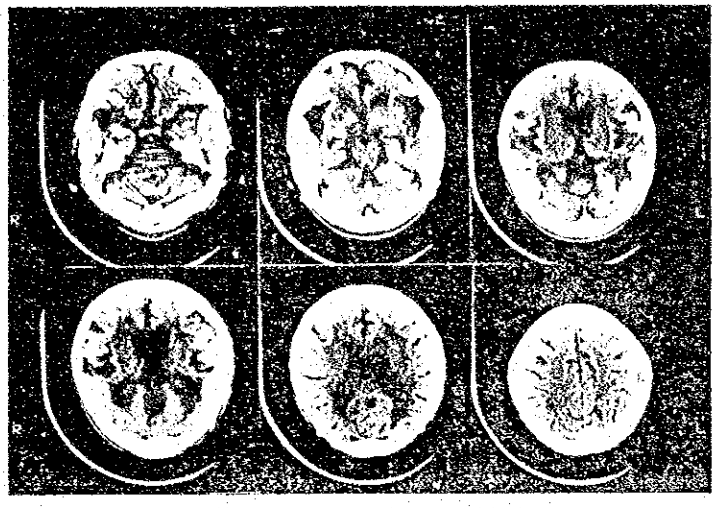

Fig 30 X-ray CT images

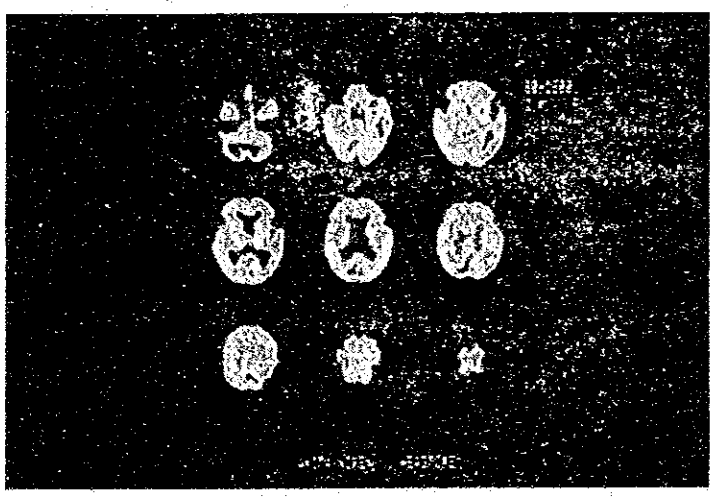

Fig 31 SPECT images using ^{99m}Tc-HM-PAO

Case 13 Pick's disease

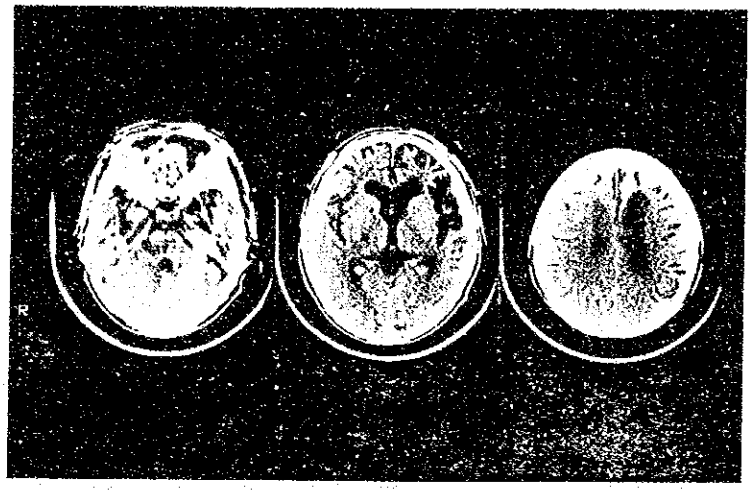

Fig 32 X-ray CT images

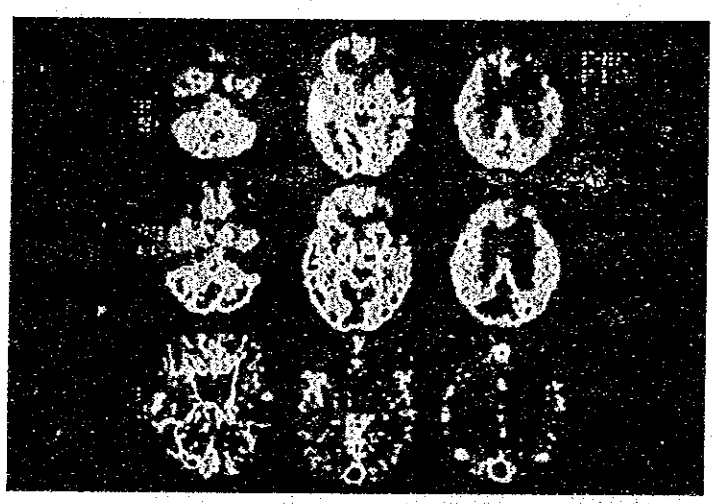

Fig 33 PET images(CBF, $CMRO_2$, CBV)

[Epilepsy]

Case 14 Epilepsy

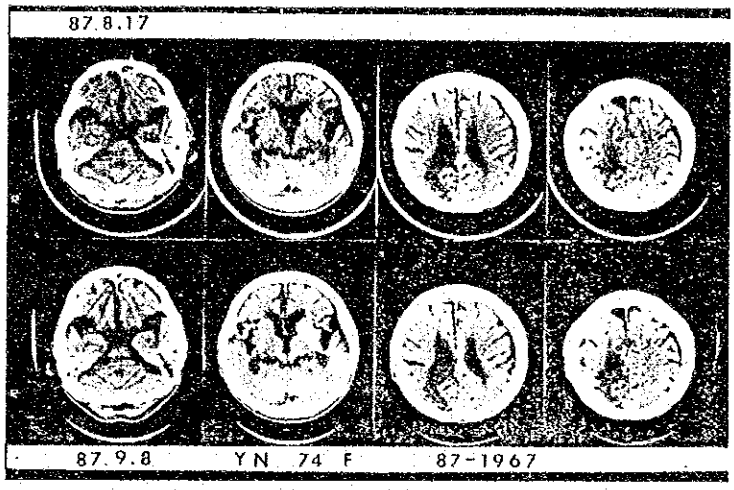

Fig 34 X-ray CT images

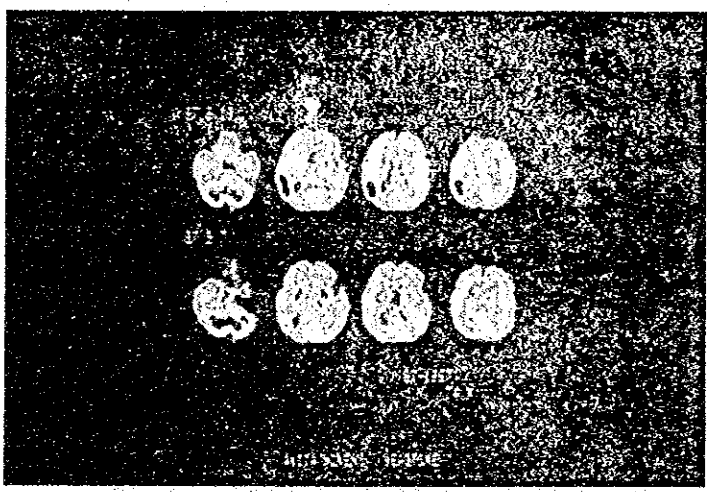

Fig 35 SPECT images using ^{123}IMP

[SCD]

Case 15 Spinocerebellar degeneration

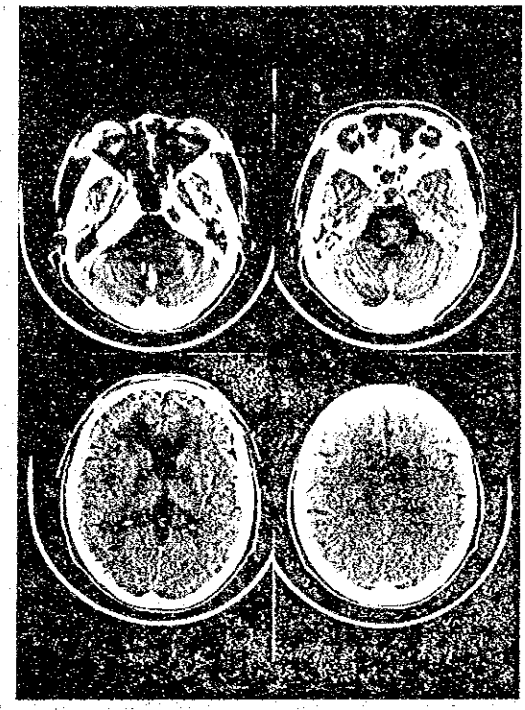

Fig 36 X-ray CT images

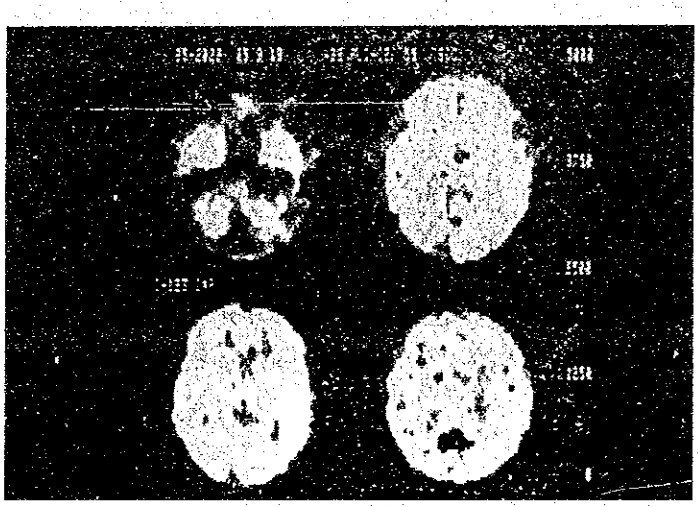

Fig 37 SPECT images using ^{123}IMP

[Herpes simplex encephalitis

Case 16 Herpes simplex encephalitis

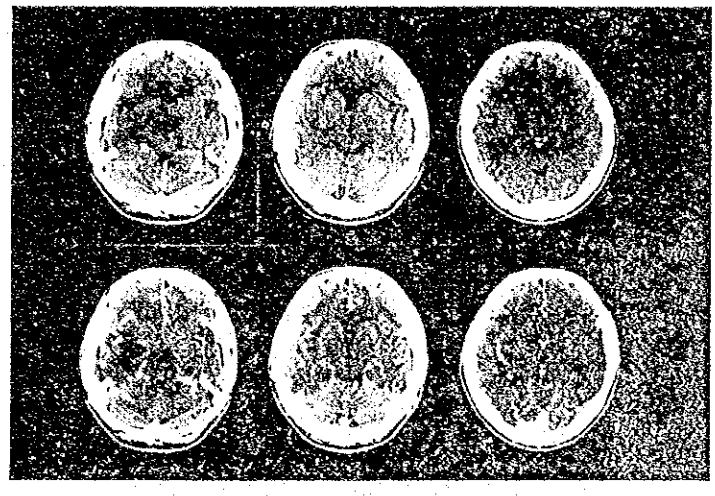

Fig 38 X-ray CT images

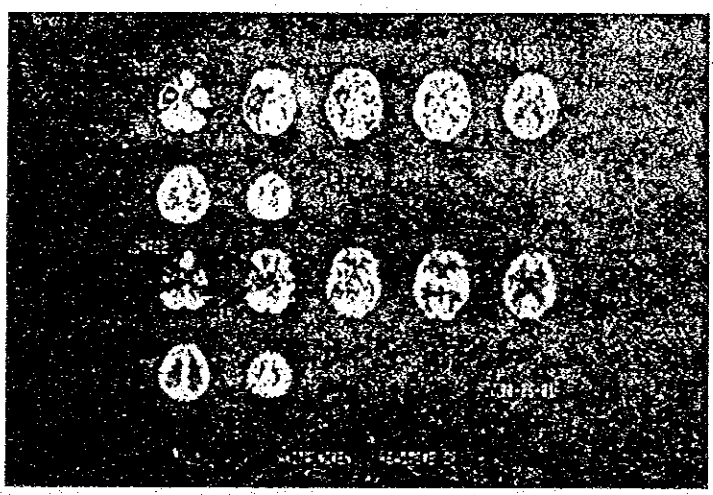

Fig 39 PET images(CBF, $CMRO_2$)

[CJD]

Case 17 Creutzhelt Jacob disease

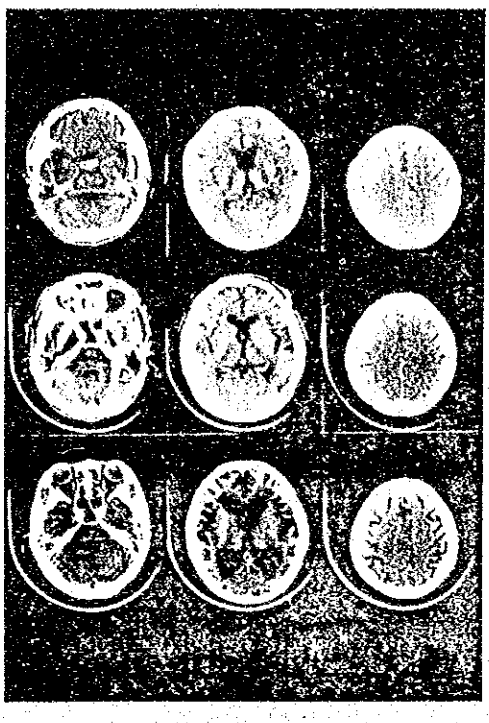

Fig 40 X-ray CT images

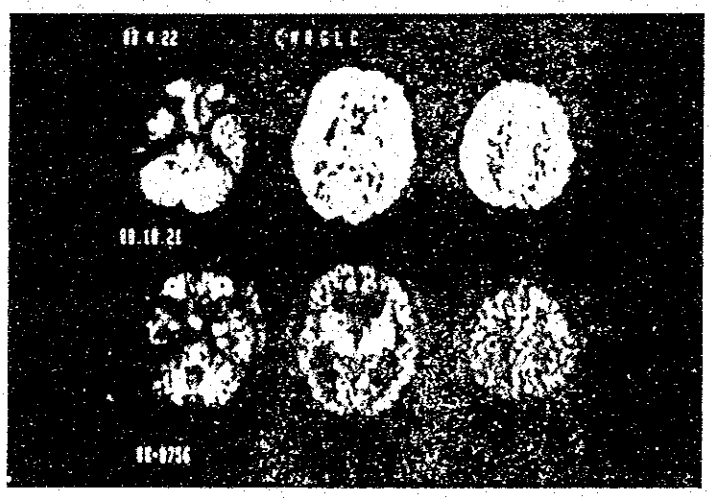

Fig 41 PET images(CMRGlc)

SEMINAR ON
NUCLEAR MEDICINE AND RADIOTHERAPY
1992 - 1993

(FOLLOW UP TEAM FOR THE GROUP TRAINING COURSE IN MEDICAL AND BIOLOGICAL APPLICATION OF RADIATION AND RADIOISOTOPES)

VOL. II (RADIOTHERAPY)

JAPAN INTERNATIONAL COOPERATION AGENCY

NATIONAL INSTITUTE OF RADIOLOGICAL SCIENCES

High dose rate remote after loading intracavitary radiotherapy for cancer of the uterine cervix: 20 years experience

Takashi Nakano, MD., Tatsuo Arai,MD., and Shinroku Morita, MD.,
Hospital, National Institute of Radiological Sciences

4-9-1, Anagawa, Inage-ku, 260 Chiba-shi, Japan

ABSTRACT

Retrospective analysis was made on 1022 patients with squamous cell carcinoma of the uterine cervix who were treated with high dose rate remote afterloading intracavitary irradiation at our institute during 15 years from 1968 to 1982 in comparison with the low dose rate intracavitary radiotherapy. They consisted of 147 patients with stage 1 disease, 256 with stage 2, 515 with stage 3 and 104 with stage 4 disease. Relative 5 year survival rates for stages 1b, 2a, 2b, 3a, 3b, 4a and 4b diseases were 90%, 80%, 70%, 59%, 54%, 25% and 14%, respectively. The rates of severe complication of Grade 3 and 4 were 4.1% for the rectosigmoid colon, 1.2% for bladder and 1.1% for small intestine. In the case of stage 1 to 2 disease, the optimal dose from intracavitary sources was suggested to be 29Gy ± 2Gy at point A with 4-5 fractions of 6-7Gy delivered over 4-5 weeks. These results suggested that high dose rate intracavitary radiotherapy provided clinical results comparable to those of low dose rate technique.

INTRODUCTION

Intracavitary radiotherapy has been recognized as one of the most effective treatment modalities for cancer of the uterine cervix. The modality generally practiced is the combination of low dose rate intracavitary radiotherapy(LICR) and the external pelvis irradiation, which have presented successful clinical results(1,2). However, this modality has some drawbacks. They are, for example, exposure of the medical staff, physical and psychological load to the patients caused by long treatment time and difficulty of keeping the precise positioning of applicators during treatment. High dose rate remote after loading intracavitary radiotherapy(HICR) was developed to overcome those drawbacks by Henschke(3) and Oconel(4) et al. in 1964 and was introduced to Japan by Wakabayashi(7) in 1965. However, the treatment was not successful in those days because of overdosage for the treatment due to ignorance of the biological response of HICR(5,6). A Japanese clinical trial of the HICR for cervical cancer patients was initiated from 1968. A correlation was demonstrated in 1978(8,9) between the optimal dose range and the fractionation(Figure 0). It also demonstrated clinical results comparable to those of LICR. Based on these results, guidelines of radiation therapy for cervical cancer were established in 1980 in Japan to standardize the treatment schedule for the intracavitary radiotherapy for cervical cancer(Table 1). At present, there are more than 150 hospitals in Japan where patients with cervical cancer are treated with HICR according to the guidelines.

The present study reports the 20 year experience and

results of the HICR for cervical squamous cell cancers in comparison with the LICR which has been previously used at our institute.

Materials and Methods

Patients

From 1968 to 1982, total of 1082 patients with cervical cancer were treated with HICR. Of these, 1022 patients with squamous cell carcinomas of the cervix were analyzed for this study excluding 60 patients with adenocarcinomas. The number of the patients of stages 1, 2, 3 and 4 diseases were 147, 256, 515 and 104, respectively. Age distribution of the patients ranged from 26 to 92 years old with mean age of 60 years old. Before 1968, 257 patients with cervical cancers were treated with LICR. The number of the patients of stages 1, 2, 3, and 4 diseases who were treated with LICR were 13, 70, 143 and 31, respectively. The mean age of the patients was 58 years old.

Radiation therapy

The radiation therapy for these patients was essentially based on the combination of intracavitary treatment and external pelvis irradiation. RALSTRON (Shimazu Cop. ltd.) system was used for HICR. TAO applicators(10) which were developed by us were combined to this machine.

The intracavitary irradiation was performed on a fractionation schedule with one insertion per week, giving 4 to 5 fractions during a period of external pelvis irradiation. Cobalt-60 sources with 2 to 4 Ci were used as the intracavitary sources. The dose rate at point A was approximately 200 to 500 rad per minute. The orthogonal x-ray films for the pelvis were

taken before each insertion and the dose at point A was calculated with these films for adjustment of total dose at point A.

External pelvis irradiation was delivered with 10 MeV photon beams or Co-60 gamma rays through 15x15 to 16x18 cm anteroposterior and posteroanterior ports. The external irradiation consisted of the whole pelvis irradiation and the pelvis irradiation with central shielding. The whole pelvis irradiation was performed with doses of 1.8Gy per fraction and 5 fractions per week. The pelvis irradiation with central shielding was performed with doses of 2 Gy per fraction and 5 fractions per week by means of central shielding with 4 cm width at midline. Over all time of the treatment ranged from 5 to 6 weeks. The treatment schedule according to the stage or the tumor volume was shown in Table 1(11). The dosage of intracavitary irradiation was coordinated according to tumor volume and microscopical tumor response as well as macroscopical tumor regression. For external irradiation, the weight of whole pelvis irradiation was increased and that of intracavitary irradiation decreased as the stage become advanced and tumor volume increased. Since 1976 when X-CT wasintroduced at our institute, paraaortic lymph node metastasis was elaborately diagnosed and was intensively treated with external irradiation with dose ranging from 50 to 55 Gy delivered over 5 to 6 weeks.

Patients follow-up

All patients treated with HTCR were followed for unlimited time from minimum of 6 years to 20 years, and those treated with LTCR followed for over 20 years. Most patients were

followed their status once a month till 1 year, once 2 to 3 months till 3 years, 2 to 3 times a year till 5 years, and once or twice a year over 5 years following radiotherapy. Additionally, over 70 % of the patients were periodically examined in in-patient clinic for complication status at 1, 3, and 5 years following treatment. The examination consisted of cystoscopy for the bladder, proctoscopy or barium enema for the colon and rectum and intravenous pyelography for the urinary tract as well as routine blood, urine and x-ray examination. Information of the patient status was obtained from our records or by letter or telephone contact with patients or their relatives.

Grading system of complication

The grading system for the complications was based on the NIRS classification(13), which was defined by modifying the Kottmeier's classification(12). The grades are as follows: grade 1 injuries signifies transient injury requiring for no or minimal medical care, grade 2 injuries requiring for continuous medical treatment,e.g. bleeding from the rectum or bladder, grade 3 injuries requiring for surgical treatment, and grade 4 injuries signifies death resulting from complication directly or indirectly.

RESULTS

Relative survivals of the patients treated with HICR according to stages are shown in Figure 1. Survival rates of 5 and 10 years after treatment were 89.5 and 77.7 for stage 1b, 79.9 and 65.5% for stage 2a, 69.7 and 60.9 for stage 2b, 59.1(5year) for stage 3a, 54.4 and 41.9% for stage 3b, 24.7 and

19.5 for stage 4a, and 13.7 and 10.6% for stage 4b disease, respectively.

For comparison, relative survivals of the patients treated with LICR according to stages are shown in Figure 2. Survival rates of 5 and 10 years after treatment were 86.5 and 89.4% for stage 1b, 88.0 and 71.5% for stage 2a, 77.3 and 68.7% for stage 2b, 49.1 and 38.0% for stage 3b, 29.7 and 14.6% for stage 4a, and 10.5 and 10.9% for stage 4b disease, respectively. Data for 3a is not available due to small number of patients. There was no significant statistical difference in the survival rates of corresponding stages between HICR and LICR groups.

Failure patterns and cause of death by stage following both HICR and LICR are summarized in Table 2. For all patients included, percentages of the patients without evidence of local recurrence and distant metastasis for stages 1, 2, 3, 4a, 4b and the total were 82, 62, 47, 22, 10 and 53%, respectively. The rates of local recurrence for stages 1, 2, 3, 4a, 4b and the total were 5, 14, 24, 33, 43, and 20%, respectively. The recurrence rates increased with the stage advancing. Similarly, distant metastasis alone significantly increased with the stage,ranging from 6% for stage 1 to 40% for stage 4b. Death from other diseases developed in 12 % of all patients. For comparison, the patterns of failure and cause of death following LICR are shown in Table 3. The failure patterns and cause of death were quite similar in corresponding stages between HICR and LICR.

The late complication induced by radiation following HICR are summarized in Table 4 according to the site. The complication rates of grade 2, 3 and 4 for the rectum and

urinary bladder conbined ranged from 5 to 7%, 2% and 2%, respectively. For the small intestine, the complication rates of the grade 2, 3, and 4 were 2, 1, and 0.1%, respectively. Table 5 shows complication rates of 257 patients following LICR. The complication rates following HICR were quite similar to these following LICR in the rectum and bladder and there was no significant difference in the complication rates between the two treatments except for the small intestine, where complications following HICR developed somewhat more than those following LICR.

Correlation between dose at point A and local control or complication in the patients with stages 1 and 2 disease, who were treated with a combination of HICR and external pelvis irradiation with central shielding are shown in Figure 3 where the dose response relationship was clearly demonstrated for both local control and complication. In this treatment schedule, probabilities of local control and complications in the rectum and bladder of these patients appeared to be associated mainly with intracavitary irradiation but not with external irradiation. Therefore, in this analysis local control was evaluated in the central lesion. Complications were evaluated in the site limited to the rectum and bladder. Additionally, complications severer than grade 2 were evaluated. Lodistic curves were best fitted for both probability of local control and complication. The dose of 50% probability for local control and complication at point A were 22Gy and 35Gy, respectively. The logistic curve for local control shows that 90% of the patients were locally controlled by dose exceeding 27Gy at point A. The curve for complication shows that 5% of

complications developed at 27 Gy and 10% of those developed at 31Gy. By compromizing the local control and the complication, optimal therapeutic dose range was estimated to be 29Gy ± 2Gy at point A for stages 1 and 2 disease.

DISCUSSION

In this report we presented clinical results of HICR for cancer of uterine cervix for past 20 years in comparison with the results of LICR performed before 1968 at our institute.

The present study indicated that the local control rates and survival rates of the HICR for 5 and 10 years after the treatment are comparable to those of the LICR. In addition, radiation induced complication rates following HICR were shown to be similar to those of LICR. It is recognized by the authors that this comparison has some limitations because the results of HICR and LICR were not obtained by randomized trial. However, our results of the HICR are comparable to those of LICR which hasbeen performed during the same period at a hospital where the treatment policy was similar to ours(14). Moreover, many results have been reported recently demonstrating the local control and complication rates of HICR comparable to those reported here(15-20). Hence, the HICR is considered to be an effective treatment modality for cancers of the uterine cervix.

Twenty years ago, many radiotherapists doubted whether the biological efficacy of the HICR was similar to those of LICR which had been practiced for long time from early 1960, although HICR had many advantages for clinical practice. Hall suggested that the biological effectiveness of high dose rate sources could be estimated by use of Ellis's NSD formula(6).

According to the formula, the biological effects of 40 Gy from low dose rate sources with 48 hours treatment was almost equal to those of 33Gy in 6 fractions with fraction dose of 5.5 Gy delivered over 12 days with high dose rate sources. This regimen was, however, difficult to practice. Moreover, HICR was regarded to be inferior to LICR in terms of therapeutic gain because of the lack of dose rate benefit for tumor control in HICR(6). However, there was no report establishing that the HICR was inferior to LICR for the treatment of squamous cell carcinomas of the cervix(16-24), although adenocarcinomas of the cervix showed some radiation resistance much more to HICR than to LICR(25).

In the early periods of introduction of HICR for the treatment of cervical cancer in Japan, there were instances whereby the patients received doses surpassing the tolerance level of surrounding tissues. This was done due to the lack of knowledge on dose rate effect(26). It resulted in many severe complications. In 1968, we initiated a Japanese trial study in order to determine optimal dose at point A for the treatment of the cervical cancer. According to the results obtained in 1978(8,9), biological effect by high dose rate sources was demonstrated to be 1.7 times higher than those by low dose rate sources. The optimal dose was estimated to be 29Gy for fraction dose of 6-7Gy, in 1 fraction per week and 4-5 fractions over 4-5 weeks, or 38Gy for fraction dose of 4-5Gy, in 2 fractions per week and 8-10 fractions over 4-5 weeks whichi is shown in Figure ##. Based on these data, we have been treating patients with cervical cancer for over 20 years. In the present study we demonstrated the dose response curves for local control and

complication from our patients following HICR and we confirmed that the optimal dose was 29 Gy ± 2Gy for stages 1 and 2 disease.

Point A dose of 30Gy in 3 fractions of 10Gy each delivered over 3 weeks, which was prescribed by Shigematsu et al.(18), appeared to be higher than optimal when compared with our results. They reported higher local control rate and higher complication. Recently, Tesima(21) reported a comparable result by treating patients with high dose rate therapy with a range of dose similar to our regimen. Neuman(17) treated the patient with high dose rate therapy by modifying a regimen of low dose rate therapy at MD Anderson Hospital using Orton & Ellis's formula. The regimen consisted of total dose of 42.5Gy at point A with 5 fractions of 8.5Gy and 1 fraction per week. They reported that local control was equivalent to that of LICR but serious complication developed in 3% of the patients. Their dose appeared to be somewhat higher than optimal dose range for Japanese patients. These suggest that there are certain problems in assessing the treatment dose only by point A dose. For example, dose distribution is different by the distance between ovoids and by the type of applicators. Radiation therapists are recommended to recognize the narrow therapeutic dose range of high dose rate treatment and to apply it with their utmost careful considerations to the dose distribution including total dose, dose rate effect, fractionation and treatment periods.

In conclusion, high dose rate intracavitary radiotherapy is one of the useful modalities for cervical cancer with many advantages for clinical practice.

REFERENCES

1. Paterson R.The treatment of malignant disease by radiotherapy. Second edition 331-359,Edward Arnold,London 1963.

2. Henschke UK,Hilaris BS, and Mahan CD. After-loading in interstitial and intracavitary radiation therapy. Am J Roent.90:386-395,1963.

3. Henschke UK, Hilaris BS, and Mahan CD. Remote afterloading with intracavitary applicators. Radiology 83:344-345,1964.

4. O'connel D, Howard N, Joslin CAF, Ramsey NW, and Liversage WE. A new remotely controlled unit for the treatment of uterinecarcinoma. Lancet, 570-571,1965.

5. Hall EJ. Radiation dose rate - a factor of importance in radiobiology and radiotherapy. Brit.J.Radiol.45:81-97,1972.

6. Hall EJ. Lethal,potentially lethal, and sublethal radiation damage and the dose rate effect. 132-169, Radiology for the radiologist.

7. Wakabayashi,M., Irie, G., Sugawara T., et al The trial production of remote after-loading system unit. Jpn J clin. Radiol 11,678-648,1966.

8. Arai T, Morita S., Iinuma T. et al. Radiation treatment of cervix cancer using high dose rate remote after-loading intracavitary irradiation. An analysis of the correlation between optimal dose range and fractionation. Jpn J cancer clin,25,605-612,1979.

9. Arai T, Morita S. Kutsutani Y et al. Relation ship between total iso-effect dose and number of fractionations for the treatment of uterine cervical carcinoma by high dose rate intracavitary irradiation. Brit. J. Rad. Special Report No17

89-92,1978.
10. Tazaki E, Arai T. Oryu S. A new applicator for intracavitary irradiation of carcinoma of the cervix. Jpn J. Radiol 10 768-775,1965.
11. Arai T., Akanuma A, Ikeda M., et al. Standardized radiation treatment method for carcinoma of the uterine cervix. Jap J. Cancer clin. 30,496-500,1984.
12. Kottmeier HL., Gray M., Rectal and bladder injury in relation to radiation dosage in carcinoma of the cervix. Am. J. Obstet Gynecol 82,74-82,1961.
13. Nakano,T., Oka,K. and Arai,T. Immunohistochemical prediction of local control of cervical cancer following radiotherapy. Int.J.Radiat.Oncol.Biol.Phys.1990 in press.
14. Arai T. Morita S. Murakami Y. et al. Local radiation complication on the irradiated carcinoma of uterine cervix. Jap. J. Clin. Radiol 26, 847-853,1981.
15. Ookawa T. Kita M. Goto etal radiation therapy alone in the treatment of carcinoma of the uterine cervix: Review of experience at Tokyo Women's Medical Collage 1969-1983. Int J Radiat . Oncol Biol. Phys. 13 1845-1849.1987.
16. Inoue T Hori S. Miyata Y et al. High versus low dose rate intracavitary irradiation of carcinoma of the uterine cervix. Acta Rad. Oncol 17, 277-282,1978.
17. Newman H. Jur B, James KW et al . Treatment of cancer of the cervix with a high dose rate after-loadiong machine(Cathetron) Int. J. Radiat Oncol Biol Phys. 9 961-937,1983.
18. Shigematsu Y., Nishiyama K., Masaki N., et al . treatment of carcinoma of the uterine cervix by remotely controlled after

loading intracavitary radiotherapy with high dose rate a comparative study with low dose rate system. Int. J. Radiat . Oncol. Biol. Phys. 9.351-356,1983.
19. Utley JF. Esen CF. Horn RA. et al . High dose rate after loading brachy therapy in carcinoma of the uterine cervix. Int. J. Radiat. Oncol. Biol.Phys. 10,2259-2263,1984.
20. Koga K. Watanabe K, Kawano M. et al. Radiotherapy for carcinoma of the uterine cervix remotely controlled afterloading intracavitary system with high dose rate. Int.J.Radiat. Oncol. Biol.Phys. 13,615-618,1987.
21. Tesima T. Chatani M. Hata K. et al . High dose rate intracavitary therapy for carcinoma of the uterine cervix. 1 general figures of survival and complication. Int.J. Radiat. Oncol. Biol.Phys. 13,1035-1041,1987.
22. Streeter OE, Goldson AL, Chevallier C. et al High dose rate Co60 remote after loading irradiation in cancer of the cervix in Haiti. 1977-1984. Int J Radiat .Oncol .Biolo.Phys. 14,1159-1163,1988.
23. Akine Y, Arimoto H. Ogino T et al High dose rate intracavitary irradiation in the treatment of carcinoma of the uterine cervix. Early experience with 84 patients. Int. J. Radiati. Oncol. Biol. Phys. 14,893-898 1988.
24. Cai Shu-Mo, Wang Xiang-E, Wang Qi, High dose rate afterloading in the treatment of cervical cancer of the uteri. Int .J. Radiat.Oncol. Biol .Phys. 16.335-338,1989
25. Arai T, Morita S. Nakano T et al Radiotherapy for adenocarcinoma of the uterine cervix. Obstet Gynecol(Tokyo) 51, 1183-1188.1983
26. Wakabayashi M. High dose rate intracavitary radiotherapy

using th Ralstron. Hokkaido Univ. School of Medi. Sapporo Japan 1971.

Legends of figures

Figure 1. Relative survivals of the patients treated with high dose rate intracavitary radiotherapy.

Figure 2. Relative survivals of the patients treated with low dose rate intracavitary radiotherapy.

Figure 3. Correlation between dose at Point A and probabilities of local control or complication in 392 patients with stages 1 and 2 diseases. Point A dose represented dose delivered from intracavitary sources.

Table 1. Treatment Protocol for Cervical Cancer

Size of tumor	External irradiation		Intracavitary irradiation	
	WP (cGy)	*CS (cGy)*	*High D-R (cGy/fr)*	*Low D-R (cGy/fr)*
Ib	0	4500	2900/5	5000/5
II				
Small	0	5000	2900/5	5000/5
Large	2000	3000	2300/4	4000/3
III				
Small	2000–3000	2000–3000	2300/4	4000/3
Large	3000–4000	1500–2500	1500/3 ~ 2400/4	2500/2 ~ 4000/3
IVa	4000–5000	1000–2500	1500/3 ~ 2000/4	2500/2 ~ 3300/3

WP: whole-pelvis field; CS: pelvis field with central shielding; D-R: dose rate; fr: fraction.

Table 2. Patterns of Failure After High-Dose-Rate Intracavitary Radiation Therapy

Stage	Patient no.	NED (%)	Rec (%)	Rec + DM (%)	DM (%)	Other (%)
I	147	82	2	3 (5)	6	7
II	256	62	10	4 (14)	11	13
III	515	47	18	6 (24)	17	12
IVa	74	22	30	3 (33)	27	19
IVb	30	10	30	13 (43)	40	7
Total	1022	53	15	5 (20)	15	12

NED: no evidence of disease; Rec: recurrence; DM: distant metastasis.

Table 3. Patterns of Failure After Low-Dose-Rate Intracavitary Radiation Therapy

Stage	Patient no.	NED (%)	Rec (%)	Rec + DM (%)	DM (%)	Other (%)
I	13	84	0	0	8	8
II	70	73	9	3 (12)	6	10
III	143	42	24	7 (31)	14	13
IVa	21	19	38	19 (57)	14	10
IVb	10	10	50	10 (60)	20	10
Total	257	49	21	7 (28)	12	12

NED: no evidence of disease; Rec: recurrence; DM: distant metastsis.

Table 4. Complication Rates of 1022 Patients After High-Dose-Rate Intracavitary Radiation Therapy

Site	Grades of severity (%)				
	0	*1*	*2*	*3*	*4*
Rectosigmoid colon	82.0	7.5	6.5	1.9	2.2
Bladder	85.3	8.0	5.5	0.8	0.4
Small intestine	95.9	1.3	1.8	1.0	0.1

Table 5. Complication Rates of 257 Patients After Low-Dose-Rate Intracavitary Radiation Therapy

Site	Grades of severity (%)				
	0	*1*	*2*	*3*	*4*
Rectosigmoid colon	70.8	10.9	15.6	2.0	0.4
Bladder	85.6	6.6	7.0	0.4	0.4
Small intestine	98.5	0.8	0	0.4	0

Fig.0 Relation between dose at point A & fractionation for high dose rate and low dose rate intracavitary irradiation.

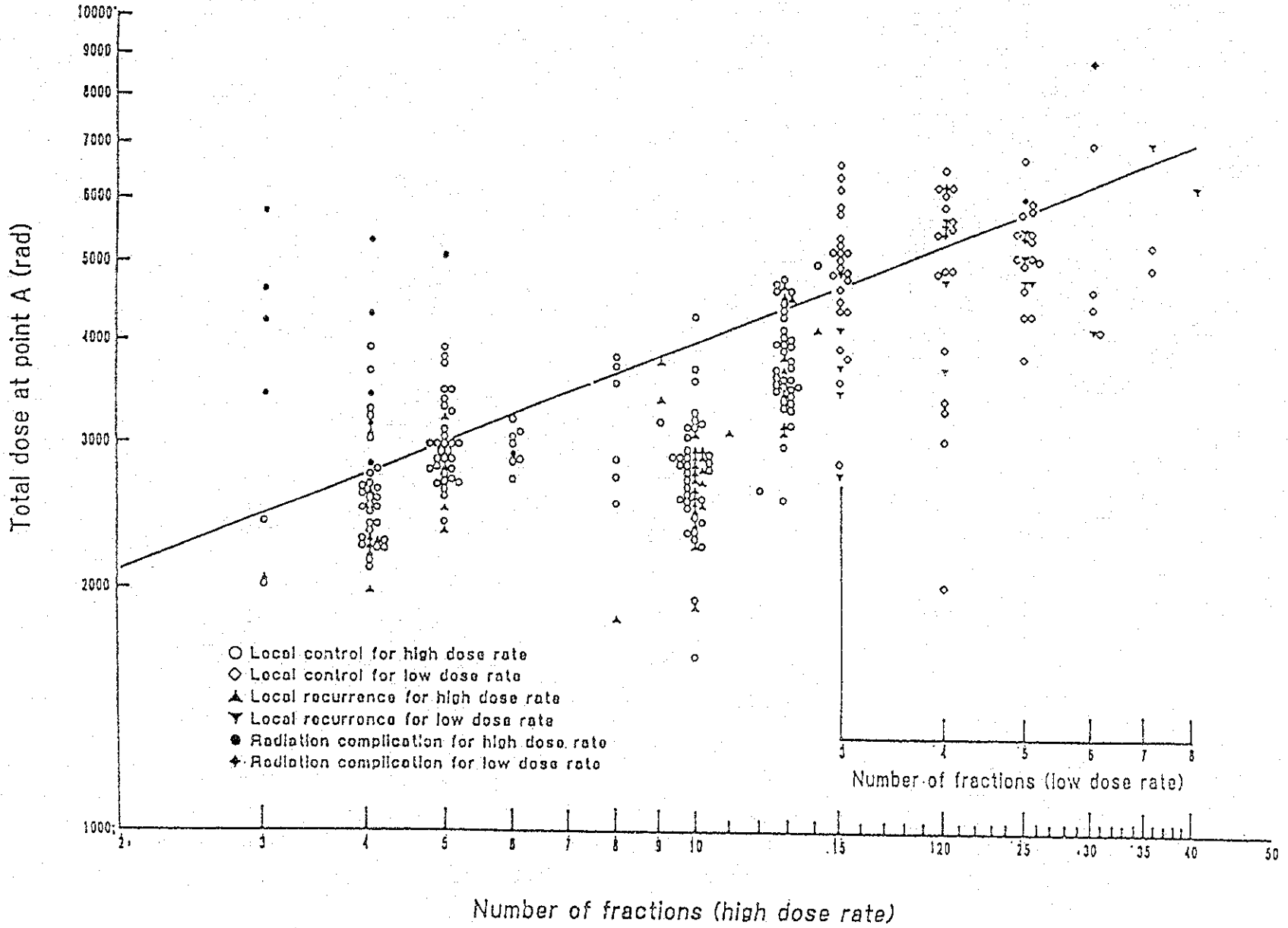

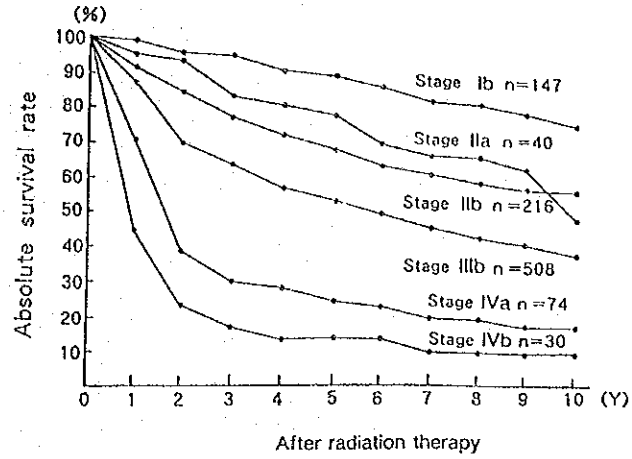

Figure 1. Absolute survival rates of patients treated with high-dose-rate intracavitary radiation therapy.

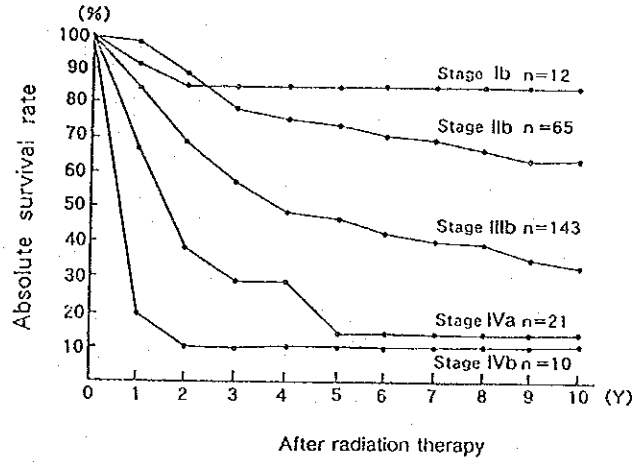

Figure 2. Absolute survival rates of patients treated with low-dose-rate intracavitary radiation therapy.

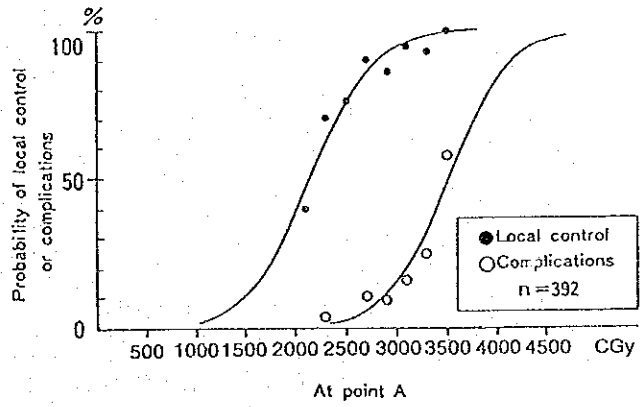

Figure 3. Correlation between dose at Point A and probabilities of local control or complication in 392 patients with Stages I and II disease. Doses at Point A represents dose delivered from intracavitary sources.